2. Appendix B

X-WiWa Deliverable 1.15
Implementation of MIKE 3

Rodolfo Bolaños, Ole S. Petersen, Henrik Kofoed-Hansen
DHI
Agern Alle 5, DK-2970, Hørsholm, Denmark

Introduction

One of the ocean-atmosphere interactions is via heat exchange where sea surface temperature (SST) plays a crucial role. The importance of the diurnal variability of sea surface temperature on air-sea interaction is being increasingly recognized. Kawai and Wada (2007) present a comprehensive review on the knowledge of the diurnal SST variation and its impact on the atmosphere and the ocean. They outline that a few numerical experiments have indicated that the diurnal SST variation can modify atmospheric properties over the Pacific warm pool or a coastal sea, but the processes underlying the modification have not yet been investigated in detail.

A 3D ocean model can be used to estimate a high temporal and spatial resolution of SST. For this purpose, the model MIKE3 has been implemented in the North Sea. This report describe the model setup and discus the model results. Results of SST have been used to assess its effects on atmospheric modelling as described in deliverable D1.16.

MIKE 3

The MIKE 3 model has been used for ocean modelling of the North Sea. The model is a component of the MIKE poweredby DHI software (MIKEbyDHI, 2014; Pietrzak et al., 2002). It is based on the solution of the three-dimensional incompressible Reynolds averaged Navier-Stokes equations, subject to the assumptions of Boussinesq and of hydrostatic pressure. The transports of temperature and salinity follow the general transport-diffusion equations (MIKEbyDHI, 2014; Pietrzak et al., 2002). The small-scale turbulence can be approximated using sub-grid scale models, several turbulence models can be applied: a constant viscosity, a vertically parabolic viscosity and a standard k-ε model (Rodi, 1984). The turbulence is described separately for the vertical and the horizontal transport. The free surface is taken into account using a σ-coordinate system but a combined σ and z-layer distribution is possible within the model. In the horizontal plane an unstructured grid is used. The spatial discretization is performed using a cell-centered finite volume method. The heat in the water can interact with the atmosphere through heat exchange. The heat exchange is calculated on basis of the four physical processes: latent heat, sensible heat, short wave radiation and long wave radiation. The model is able to also take into account tidal potential (Pugh, 1987), evaporation/precipitation, wind stress, 2D wave radiation stresses and the open boundaries can be forced by elevation, velocity, salinity and temperature. Wind stress is based in a drag formulation dependent on wind speed (Wu, 1984).

Model domain

The model domain covers the North Sea, Norwegian Sea and Barents Sea. The most northern latitude of the domain is at 81° N and the most southern lies at 47.9° N. The western limit is delimited by 4.5° W and the eastern one by 47.8° E as seen in Figure 1. The mesh resolution

goes from 0.2 degrees in the most offshore part of the Norwegian Sea up to 0.05 degrees in the coastal part of the southeast North Sea. In the vertical the models uses a combined sigma and z-levels. With 13 sigma levels in the top 61 m and 20 z-levels underneath with a variable vertical distribution.

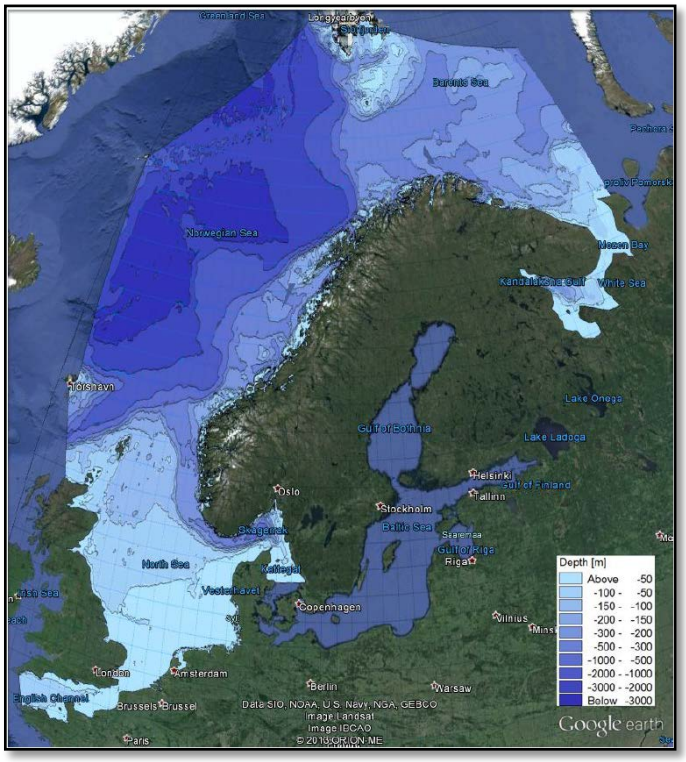

Figure 1- Model domain

Ocean boundary forcing and initial conditions

A downscaling approach has to be used to model the 3D ocean dynamics of the North Sea with high spatial resolution. This requires the generation of open boundaries and initial conditions derived from global ocean models. MyOcean data (now Copernicus) has been used to providing temperature, salinity and large scale (not tidal) surface elevation and ocean currents to MIKE 3.

My-Ocean

Operational Oceanography has been acknowledge by the European Commission as one of the 3 key-domains covered by its GMES program. As a consequence, the European Commission co-funded a 3-year period called My Ocean in the 7th framework program for European research and Development. This project was undertaken in April 2009 and came to an end on March 2012. It was dedicated to the preparation of GMES (Global Monitoring for Environmental and Security). It had a free access and provided state-of-the-art information available on the global ocean based on the combination of space and in situ observations and their assimilation into 4D models. Some of the variables available are temperature, salinity, currents, sea ice, sea level, wind and biogeochemical parameters. These models rely on the aggregation of Eu-

ropean modelling tools and the scientific methodology is a result of a strong collaboration between operational and research communities. The continuation of the efforts done by MyOcean are being carried out by Copernicus (http://marine.copernicus.eu/)

Tidal forcing

Tidal currents and surface elevation variations are included in the downscaling methodology. A 2D tidal simulation is done by imposing a tidal surface elevation in the model boundaries, this 2D model run generates the tidal boundary currents that are used to force the 3D model in combination with the baroclinic current provided by MyOcean data. The tidal surface elevation is produced by the DTU10 (altimetry based) global tidal model (Chen and Andersen, 2010), which is part of the MIKE Powered by DHI software tools.

Atmospheric forcing

The atmospheric forcing employed was provided by the WRF model as implemented by StormGeo and included hourly fields of clearness coefficient, air temperature, humidity, precipitation, atmospheric pressure and wind velocity components with a spatial resolution of 0.1 degrees. Figure 2-4 show and example of the wind speed components and air temperature during the storm that occurred in the North Sea on the 27/11/2011. It can be seen that modelled wind reach 25 m/s while the air temperature distribution shows a warmer air south of Ireland an UK.

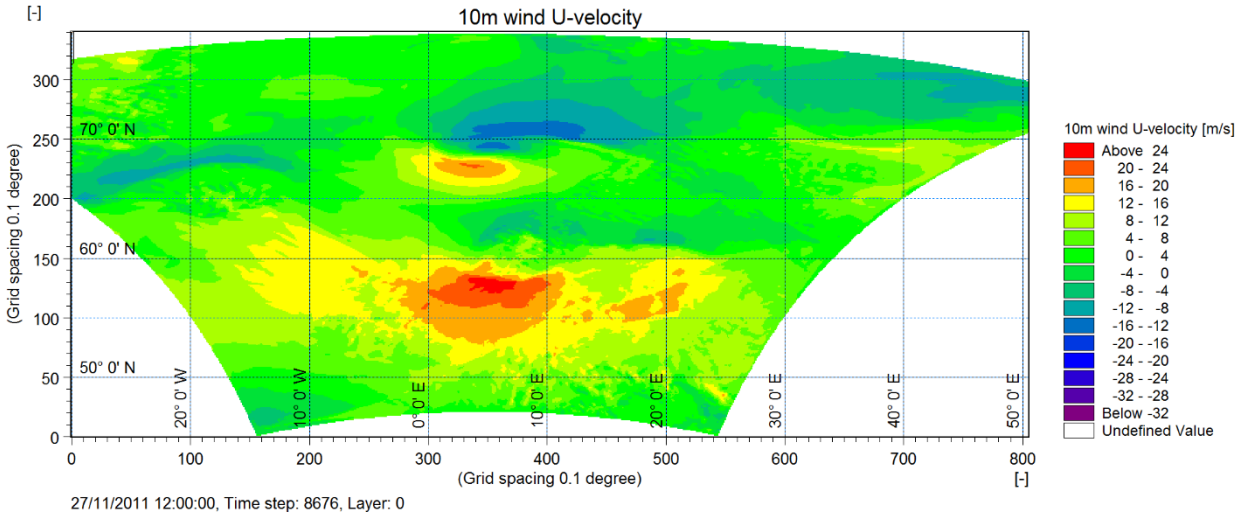

Figure 2. Zonal component of wind during the wind event on the 27/11/2011 in the North Sea.

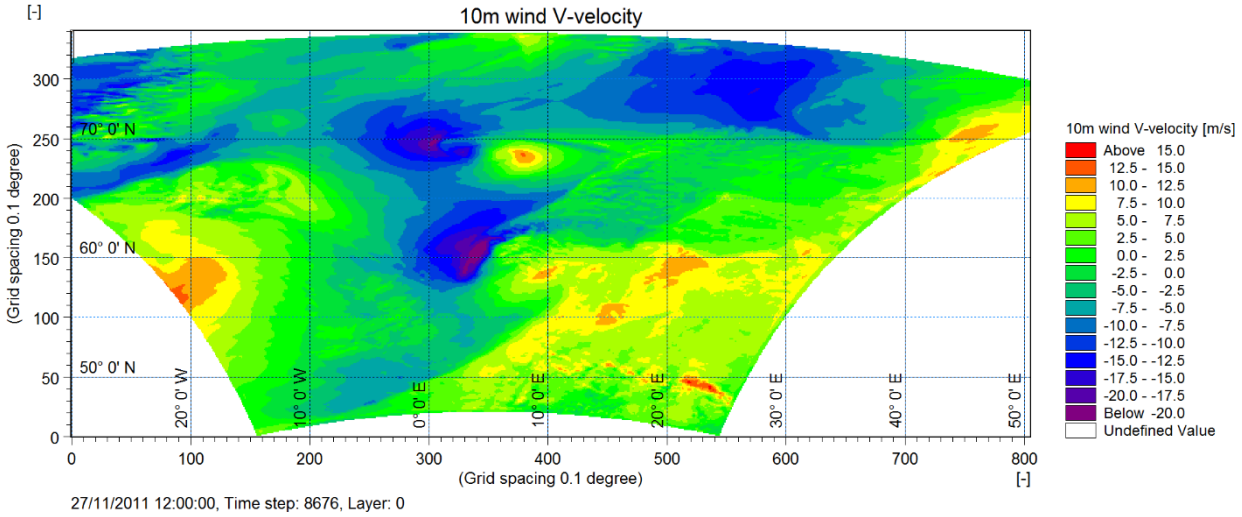

Figure 3. Meridional component of wind during the wind event on the 27/11/2011 in the North Sea.

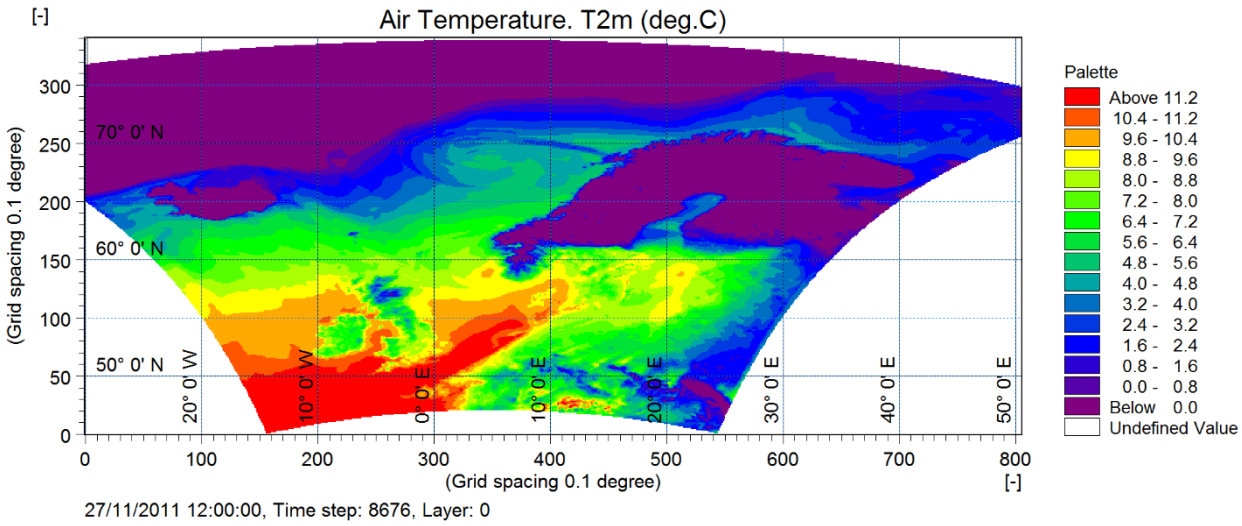

Figure 4. Air temperature during the wind event on the 27/11/2011 in the North Sea.

Measurements data

Sea surface temperature

Sea surface temperature measurements from satellite are used to validate model results. Data is provided as a grid of ¼ degree resolution with one temperature field per day. Measurements were taken with the Advanced Very High Resolution Radiometer (AVHRR) and Advanced Microwave Scanning Radiometer (AMSR) on the NASA Earth Observing System satellite. It uses in-situ data from ships and buoys and includes a large-scale adjustment of satellite biases with respect to the in-situ data (Reynolds et al., 2007). Data is available at http://www.ncdc.noaa.gov/data-access/satellite-data/satellite-data-access-datasets. Figure 5 shows an example of the satellite data used for model validation in the North Sea.

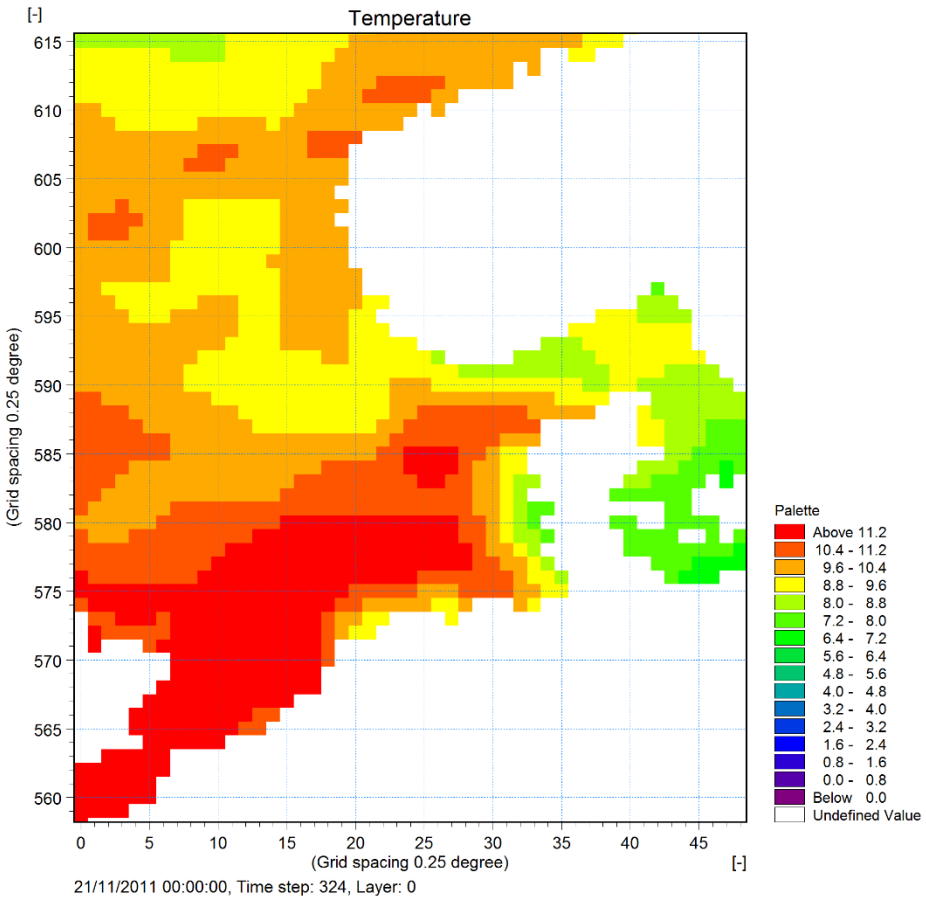

Figure 5. Satellite sea surface temperature data in the North Sea on the 21/11/2011.

ADCP

An Acoustic Doppler Current Profiler (ADCP) deployed by Statoil at Heimdal station is used to perform an assessment of the model for the period of September 2011 to December 2011. The location of Heimdal is at 2.23° E 59.58° N at a water depth of 118 m. Data at three different water depths are used to assess model results in term of current speed and direction.

Model results

Output of the ocean model is 3D fields of salinity, temperature, and current components as well as 2D fields of depth averaged current and surface elevation. Figures 6 show an example of the distribution of surface currents on the 21st November 2011, large velocities can be seen in the English channel and surrounding areas mainly triggered by tides. Figure 7 shows the spatial distribution of salinity where the contribution of fresh water from the Baltic Sea is clearly shown. Figure 8 shows sea surface temperature, where warmer water coming from the English Channel and colder from the Baltic Sea are appreciable.

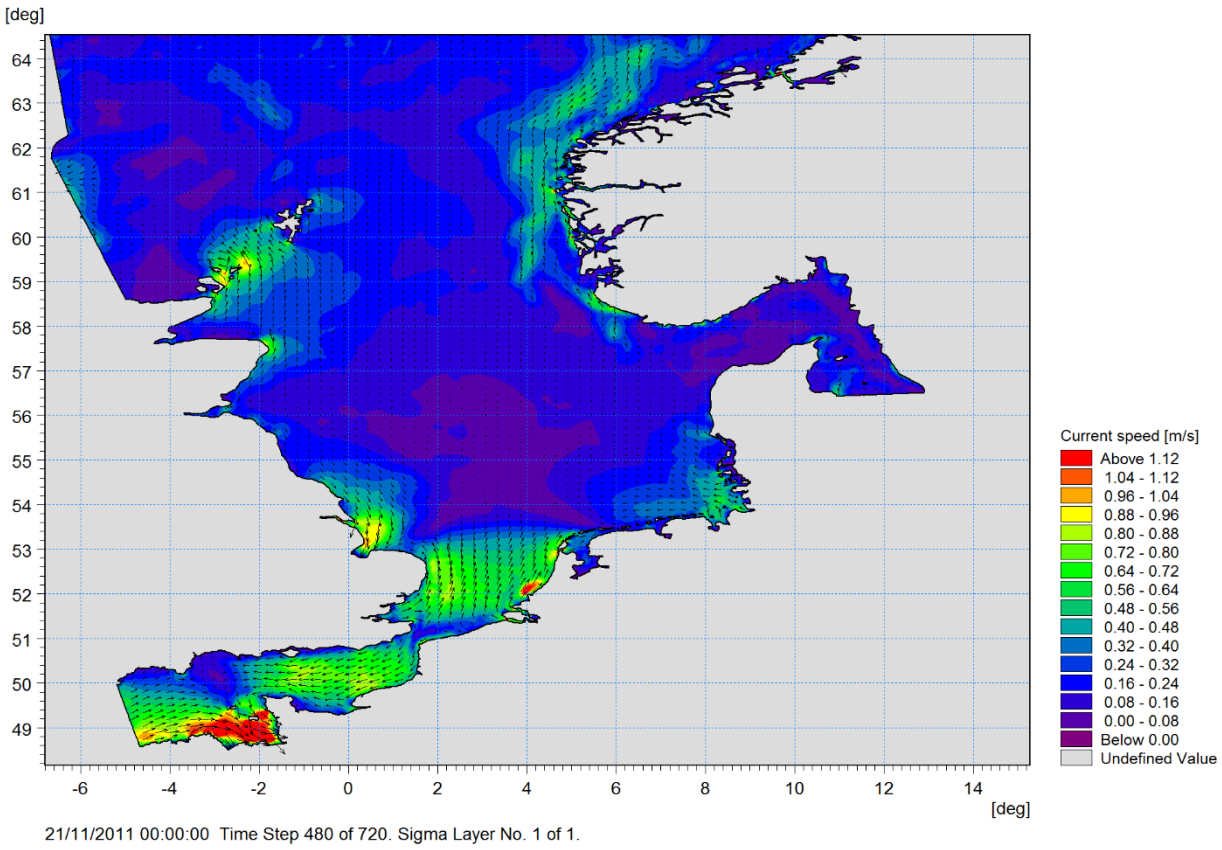

Figure 6 Spatial distribution of surface currents on the 21 Nov 2011

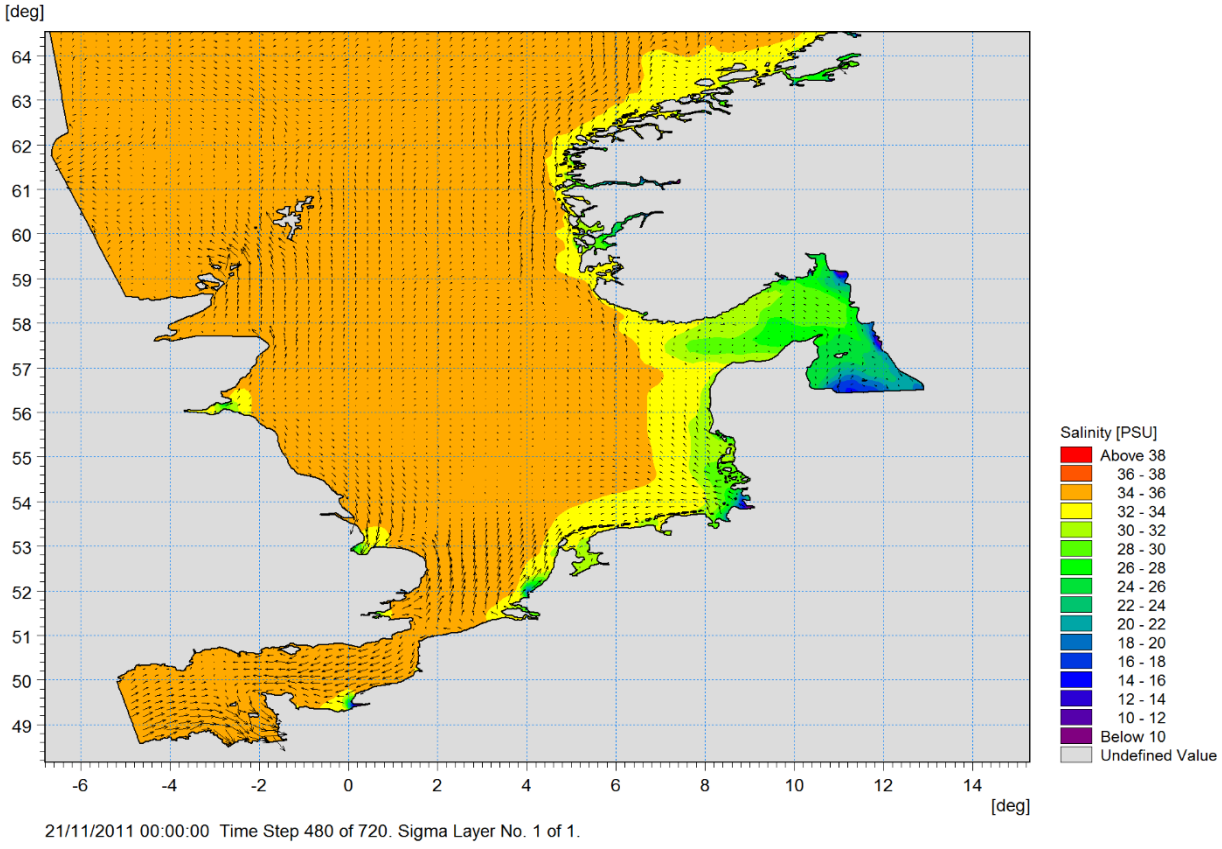

Figure 7. Spatial distribution of salinity on the 21 Nov 2011

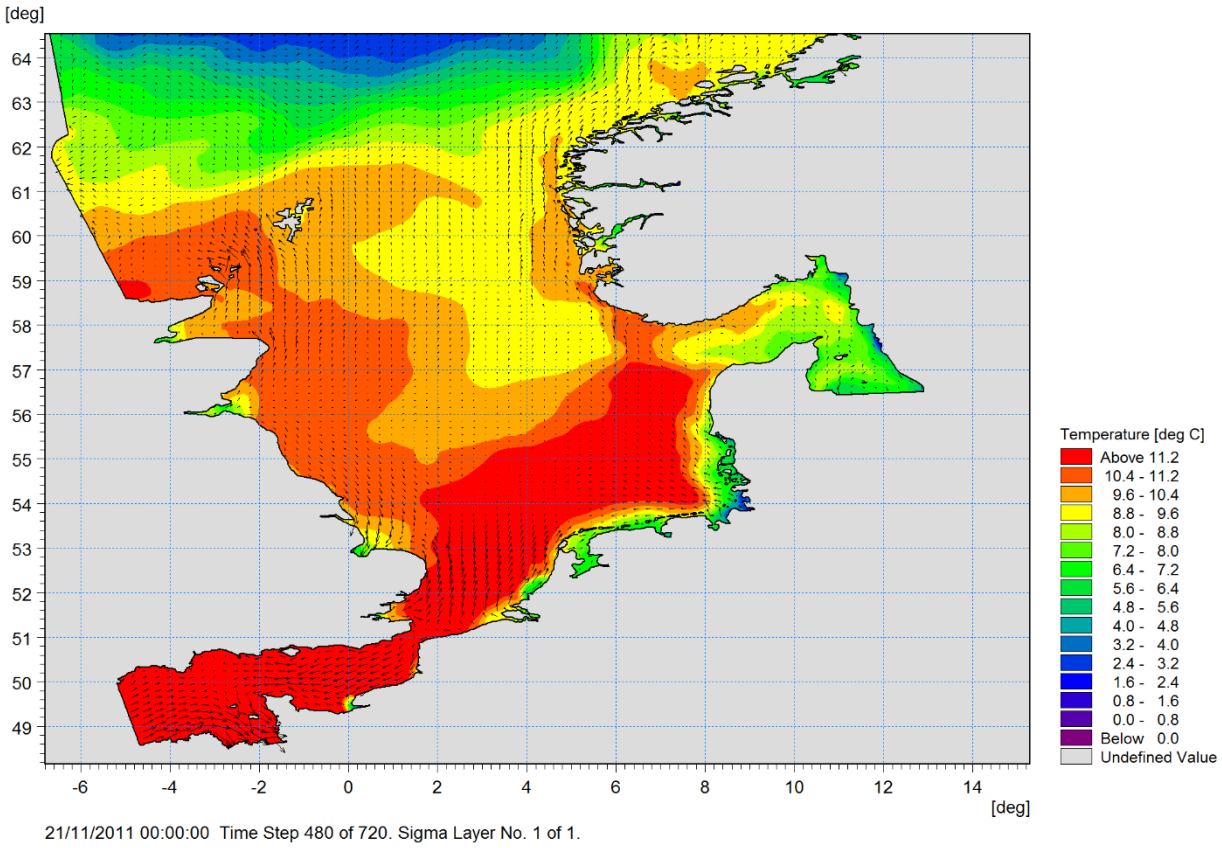

Figure 8. Spatial distribution of sea surface temperature on the 21 Nov 2011.

SST validation with satellite data

Figure 9 shows the location of six points used to extract time series (figure 10) of SST for November 2011. The SST shows a decrease in the first 23 days of the month, in agreement with the seasonal cooling down and with satellite data. The model time series show high temporal (higher than daily) oscillations reaching variation of up to 1 degree, that are associated to tidal advection and not due to diurnal warming. The comparison of the model SST time series with the satellite shows the good agreement of features and also outlines the richness of model data which shows significant spatial differences.

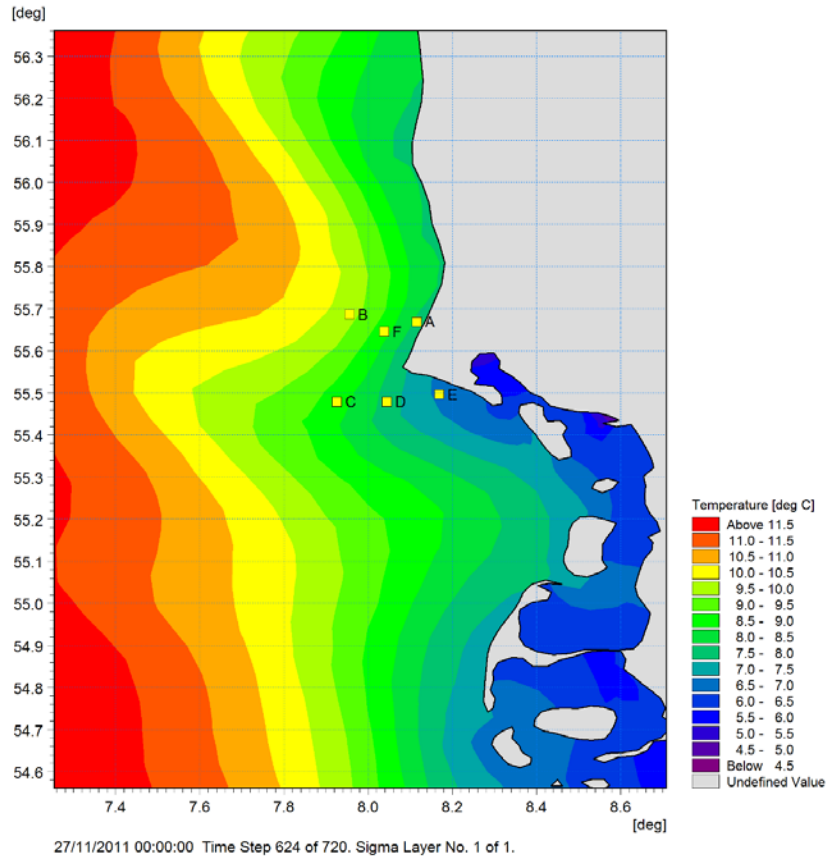

Figure 9. Location of 6 points used for time series of SST near Horns Rev depicted in figure 9.

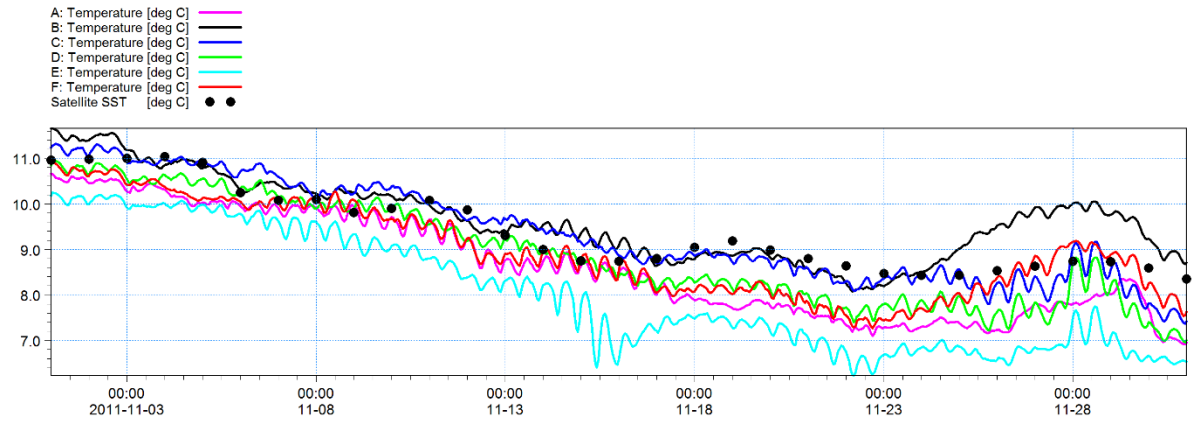

Figure 10. Time series of model SST at the six points depicted in figure 9 and satellite SST.

Figure 11 shows the evolutions of the spatial model skills statistics (Bias, RMSE, SI, and correlation coefficient) along the year when comparing sea surface temperature (SST) at the grid points of the satellite data within the North Sea (up to 60^{o} N). Top model layer (~ 1 m thickness) has been used for comparison. The figure shows a seasonal behaviour of the model skills, producing larger errors during summer when model underestimates surface temperature, thus producing a negative bias and an increase in the RMSE.

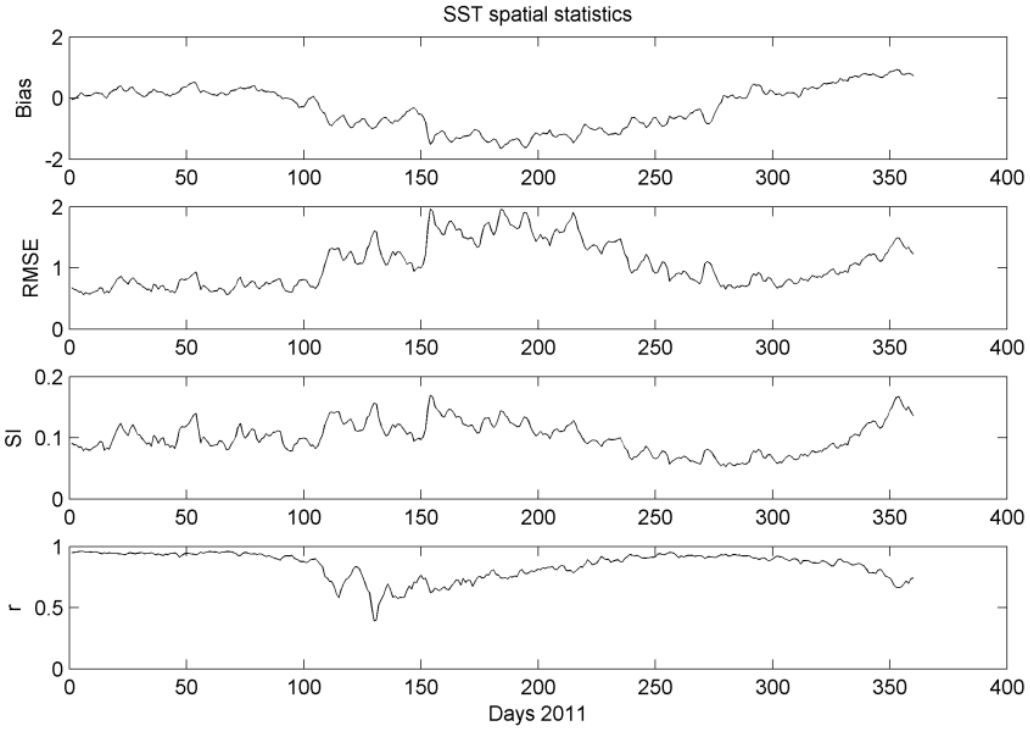

Figure 11. Sea surface temperature model statistics time series when compared with satellite measurements in the North Sea for 2011.

Currents validation with ADCP data

Ocean current modelling in the continental shelf can be a challenge due to the generation and propagation of mesoscale vortices that, if modelled in slightly wrong position, can produce apparent large errors when comparing with observation. The model was able to, in general sense, reproduce the current speed and direction at Heimdal. Figure 11 shows a time series of modelled and measured current speed and direction. It can be observed that the model, although not perfect, simulates the temporal variation of speed and direction as well as the vertical variations which present different features along the water column.

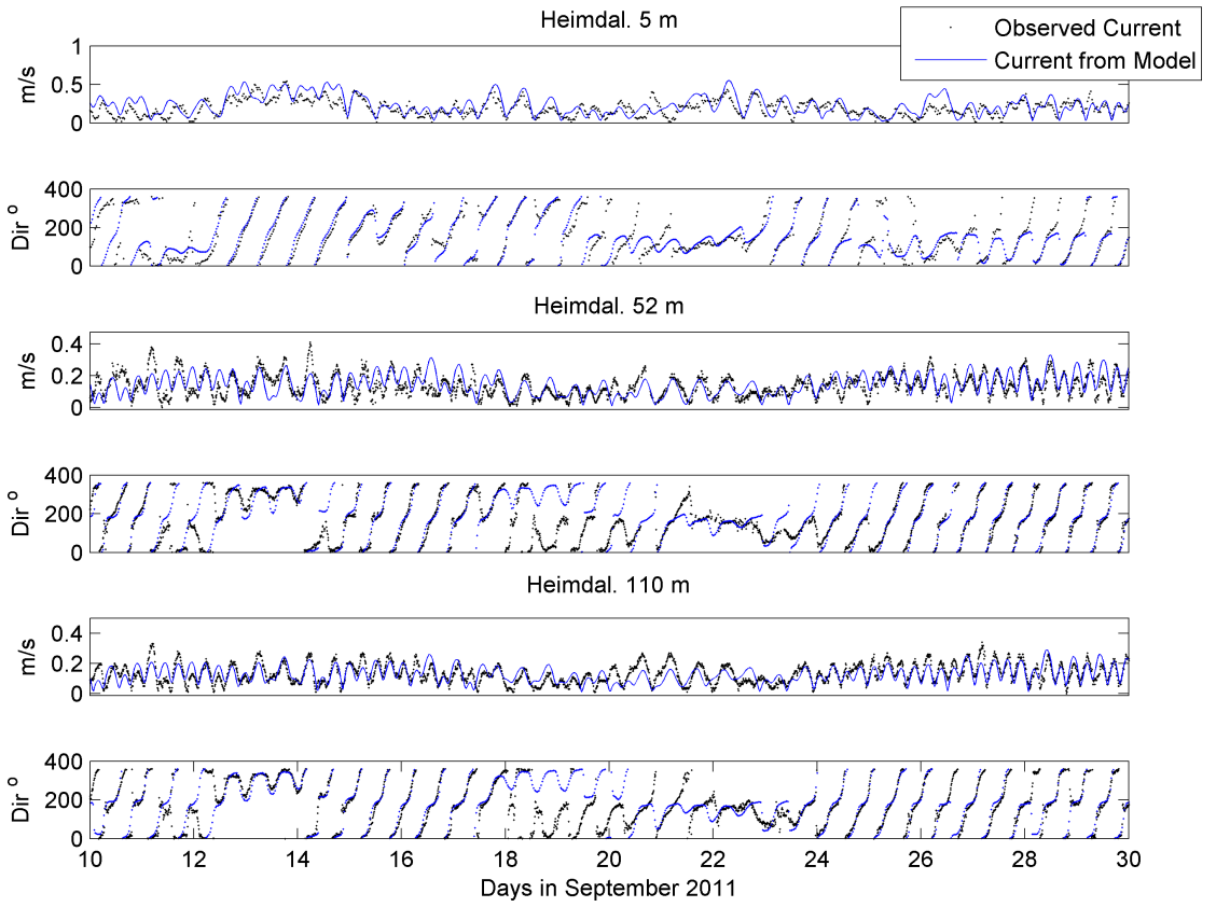

Figure 12. Time series of modelled (blue) and measured (black circles) currents speed and current direction at Heimdal at three different water depth (5, 52 and 110 m).

Discussion

The implementation of MIKE 3 for the North Sea provided very good results in term of the ocean currents at the validation point (Norwegian Sea). This can be very site dependent and evaluation at other areas within the domain should be performed in order to provide a more comprehensive assessment of model results. Hydrodynamic at sites, such as Horns Rev, that present a complex and shallow bathymetry would require a detailed and specific high resolution model in order to reproduce the local currents features product of the combination of tides, baroclinic and bathymetric induced flows.

In terms of the sea surface temperature the model also presented good results, and although some bias with the satellite data was obtained the model allow us to assess the impact of high resolution SST in the atmospheric model WRF during a wind event.

The model results presented high frequency oscillations (semidiurnal) of SST associated to tidal processes giving changes of to 1 degree within 1 day. This also points out to the spatial gradients, as it is the tidal advection moving spatially the SST field.

The response of WRF to the SST from MIKE is discussed in deliverable D1.16, its effect was mainly observed at the air temperature, and the difference of WRF results between using a daily value from standard WRF and an hourly value from MIKE seems to be due to the difference in temperature magnitude and not due to the higher temporal oscillations reproduced by

MIKE and not captured in the daily values. These oscillations in SST seemed not to be of significance for the storm case tested, although some changes were noticed in the coastal location. In deliverable D1.16 it has been identified six cases with large warming diurnal events around Denmark. However, it seems that they occurred during low wind conditions and, although significant impact of using a high resolution SST could be expected, this will not have an implication for extreme wind conditions.

Final concluding remarks

- Model reproduce current features at Heimdal station
- Model presents SST semidiurnal variation of up to 1 degree related to tidal advection
- Modelled SST reproduce seasonal patterns
- Model SST has been used for atmospheric modelling as described in deliverable D1.15

Acknowledgments

Authors thank STATOIL for providing ADCP data. *MyOcean* (now *Mercator*) is also acknowledge for providing the ocean data used in this study. Authors tank continuous interactions with other DHI colleagues (Morten Rugbjerg, Jacob Tornfeldt, among others) during the development of this work.

References

Bleck, R., 2002. An oceanic general circulation model framed in hybrid isopycnic-Cartesian coordinates. Ocean Modelling 4, 55-88.

Cheng, Y., Andersen, O.B., 2010. Improvement of Global Ocean Tide Models in Shallow Water Regions, Altimetry for Oceans and Hydrology OST-ST Meeting.

Halliwell, G.R., 1998. Simulation of North Atlantic decadal/multi-decadal winter SST anomalies driven by basin-scale atmospheric circulation anomalies. Journal of Physical Oceanography 28, 5-21.

Halliwell, G.R., R., B., Chassignet, E.P., Smith, L.T., 2000. Mixed layer model validation in Atlantic Ocean simulations using the Hybrid Coordinate Ocean Model EOS 80, OS304.

MIKEbyDHI, 2012. MIKE 21 & MIKE 3 flow model FM. Hydrodynamic and Transport Module. Scientific Documentation. DHI, Hørsholm, Denmark, p. 50.

Pugh, D.T., 1987. Tides, surges and mean sea-level: a handbook for engineers and scientists. Wiley, Chichester.

Pietrzak, J., Jakobson, J.B., Burchard, H., Vested, H.J., Petersen, O.S., 2002. A three-dimensional hydrostatic model for coastal and oceanmodelling using a generalised topography following co-ordinate system. Ocean Modelling 4, 173-205.

Reynolds, R.W., Smith, T.M., Liu, C., Chelton, D.B., Casey, K.S., Schlax, M.G., 2007. Daily high-resolution blended analyses for sea surface temperature. Journal of Climate 20, 5473-5496.

Rodi, W., 1984. Turbulence models and their application in hydraulics, in: IAHR (Ed.), Delft, p. 104.

3. Appendix C

X-WiWa Deliverable 1.16
Sensitivity of the heat transfer during extreme events
Sea surface temperature experiments

Rodolfo Bolaños[1], Iona Karagali[2], Jianting Du[2], Xiaoli Larsen[2], Mark Kelly[2]

[1] DHI, Agern Alle 5. DK-2970 Hørsholm
[2] Wind Energy DTU Risø.

1. Introduction

One of the ocean-atmosphere interactions is heat exchange, where sea surface temperature (SST) plays a crucial role. The sea surface is the lower boundary of the atmosphere and SST is an important environmental variable, partly controlling the exchange of heat and gases between the ocean and the atmosphere, of importance for weather and climate. The temperature of the ocean is known to vary over longer time scales compared to the atmospheric temperature, due to the larger heat capacity of the water. Nonetheless, SST refers to the upper oceanic temperature; due to stratification and the immediate response to atmospheric forcing, it has much higher temporal variability compared to the deeper layers.

During day time and given the existence of favourable conditions, i.e. low winds and solar heating, the upper few meters of the oceanic layer undergo warming that can reach up to several degrees. Most of this energy is contained within the top few millimetres of the water, i.e. the part observable from microwave and infrared sensors on space-borne platforms. Diurnal SST variability has been observed in different areas of the global ocean (Price et al., 1987; Ward, 2006; Merchant et al., 2008) using combinations of in situ and satellite observations. Recently, large diurnal warming signals were revealed in the inter-tropical Atlantic (Le Borgne et al., 2012) while diurnal warming has also been reported at higher latitudes (Eastwood et al., 2011; Karagali et al., 2012). The effect of the diurnal sea surface warming on the sea breeze circulation is expected to obtain over other coastal areas throughout the world, especially in the tropics (Kawai and Wada, 2007).

Atmospheric, oceanic and climate models are currently not adequately resolving the daily SST variability, resulting in biases of the total heat budget estimates (Webster et al., 1996; Ward, 2006; Bellenger and Duvel, 2009; Bellenger et al., 2010) and therefore, demised model accuracies. For example, the diurnal temporal increase of the net surface heat flux from the ocean can exceeds 10 W/m^2 which is non-negligible for the atmosphere (Kawi and Wada, 2007). Strong SST diurnal signals can complicate the assimilation of SST fields in ocean and atmospheric models, the derivation of atmospheric correction algorithms for satellite radiometers and the merging of satellite SST from different sensors (Donlon et al., 2007). Not accounting for the daily SST signal can cause biases in the scatterometer derived ocean wind fields and biases in the estimated net flux of CO_2, as the out flux of oceanic CO_2 is positively correlated with the increase of SST.

Previous work has focused on analysing the diurnal variability of SST using satellite observations from a geostationary platform obtaining hourly SST retrievals over the Atlantic Ocean and the European Seas (Karagali and Høyer, 2014). Large events occurred during the spring and summer period at both coastal and open ocean waters. Especially for the North Sea and the Baltic Sea, the highest peak of the diurnal SST cycle was identified, reaching a mean noon maximum of 1.4 degrees higher compared to the early morning values.

Based on such findings and the importance of SST in atmospheric modelling, it is relevant to investigate the impact of resolving the daily SST cycle in an atmospheric model. A 3D ocean model can be used to estimate a high temporal and spatial resolution of SST. For this purpose, the model MIKE3 has been implemented in the North Sea as described in the deliverable D1.15 of the X-WiWa project.

1.1. SST high resolution measured and reanalysis data

1.1.1 MSG/SEVIRI SST

The Spinning Enhanced Visible Infrared/Microwave Imager (SEVIRI) is on board the Meteosat Second Generation (MSG, MSG-2) satellites. As an infra-red instrument it has no cloud penetration skill. Being in geostationary orbit centered at zero degrees latitude and longitude and with a nominal resolution of 0.03 degrees it records information every 15 minutes, on a circular domain extending from 60^{o} South to 60^{o} North and from 60^{o} West to 60^{o} East. Measurements are averaged in hourly intervals and are interpolated to a 0.05 degree grid.

SEVIRI hourly fields from Centre Météorologie Spatiale (CMS), Météo France were obtained for the period 2006-2012. The SEVIRI SSTs are corrected for the cool skin bias by adding 0.2 K in the original skin retrievals and are therefore representative of sub-skin temperatures.

MSG/SEVIRI SST retrievals are classified using a quality flag index that ranges from 0 (unprocessed), 1 (erroneous), 2 (bad), 3(acceptable), 4 (good) to 5 (excellent). In addition, a missing reason flag is available, which indicates the reason for the unprocessed data that are quality flagged with 0. The values of the missing reason flag range from 0 (no data), 1 (out of area), 2 (aerosol), 3 (cloud mask), 4 (cloud time variability), 5 (cloud climatology), 6 (ice), 7 (other) to 8 (quality control).

1.1.2 DMI North Sea/Baltic Sea SST Re-Analysis

The Danish Meteorological Institute (DMI) produces a daily optimally interpolated SST field, from blended satellite and in situ observations, specifically designed for the North and Baltic Seas. The method used to generate this product is described in Høyer and She (2007). Data is available from 1982 onwards at a spatial resolution of 3 km.

2. Other heat exchange processes

Janssen (1997) studied the sea state dependence of heat and moisture flux, finding that the effect was small compared to the effect on the momentum, because both the Stanton number and the Dalton number depend on the square root of the drag coefficient.

Andreas and DeCosmo (2002) suggested that the spray effects are most evident in the latent heat flux data, where spray contributes roughly 10% of the total turbulence flux in the winds of 10 m/s and between 10 and 40% in the winds of 15-18 m/s. Many numerical studies have used the spray mediated transfer functions for sensible and latent heat developed by Andreas et al.

(2008) to examine how the implementation of the spray effect affects the drag coefficient and wind field for storm and hurricane wind strength (e.g. Liu et al. 2012; Zhang et al., 2006; Wu et al. 2015).

Andreas et al. (2015) present an updated algorithm for air-sea surface flux including sea spray. They introduced a new drag relation (Andreas et al., 2012) that naturally provides a non-zero surface stress even at zero average wind speed and has better properties than the Charnock relation when extrapolated beyond winds of 30 m/s. They also presented some validation for winds up to 25 m/s, but they suggest that the extrapolation of their drag relation is acceptable for hurricane winds, as it is consistent with theory (e.g. Moon et al (2007) and Mueller and Veron (2009)). Limiting the value of the drag coefficient in high winds to values much less than those predicted by the Charnock relation, seems to have improved hurricane models (e.g., Tang and Emanuel, 2012; Jarosz et al., 2007; Sanford et al., 2007; Chiang et al., 2011) which also is in agreement with the limiting value that has been used for wave modelling under hurricane winds (Jensen et al., 2006; Fan et al., 2012). It is also worth noting that the Andreas *et al.* (2012) drag formulation does not consider the roughness variable, avoiding the uncertainties in formulations of z0, including the severe self-correlation resulting from attempts to evaluate its behaviour from data (e.g. Vickers *et al.*, 2015; Mahrt *et al.*, 2003; Janssen, 1997).

The Andreas et al. (2015) formulation includes both spray and interfacial contributions in fluxestimates, and could explain for all wind speeds both the magnitude and the wind-speed dependence of the measurements. This analysis allows separation of the measurements into interfacial and spray contributions. In their analysis and in the resulting bulk flux algorithm, there is no explicit coupling between the interfacial processes and the spray processes. While this iteration would be straightforward, it would introduce complexity that seems unjustified in light of the various uncertainties in the understanding of spray processes. They did not find the arguments for spray to affect atmospheric stratification very compelling. The authors argue that previous analyses that do suggest dynamically important spray effects on stratification usually assume spray mass loadings that are unrealistically large (e.g., Pielke and Lee, 1991; Barenblatt et al., 2005) or spray generation rates that vary as very high powers of wind speed (as u^5_* in Kudryavtsev (2006)) and therefore do not appear consistent with dimensional analysis and energy conservation arguments (e.g. Emanuel, 2003).

3. The ocean model. MIKE 3

The MIKE 3 ocean model has been implemented for the North Sea using *MyOcean* data as initial and boundary conditions. Details on the model description and validation can be found in the deliverable D1.15 of the X-WiWa project.

The MIKE 3 implementation allows the generation of SST fields with high spatial and temporal resolution. Modelled (hourly) SST has been used as an input to the atmospheric model WRF to be able to assess if there is any benefit from the high temporal resolution instead of the commonly used daily values. The period was November 2011, which present a strong wind event reaching up to 20 m/s within the North Sea with waves of about 6 m Hm0.

4. The atmospheric model. WRF

In this study, WRF runs on three nested domains for November 2011, covering the region shown in Fig. 1. The horizontal resolution of the first, second, and third domain is 18 km, 6 km, and 2 km respectively. Each domain has 46 vertical sigma levels with the lowest level height at about 10 meters. The MYNN 3.0 (Nakanishi and Niino, 2006) planetary boundary layer (PBL) scheme for turbulence and (subgrid) fluxes, Thompson et al. (2004) microphysics scheme for phase change, and RRTM (Iacono et al., 2008) long-wave and short-wave radiation physics schemes are used in all the three domains. The Kain and Fritsch (1993) cumulus scheme is used for the first and second domains, while for the third domain the cumulus scheme is turned off. The COARE3.0 (Fairall et al., 2003) formulation is used for the calculation of aerodynamic, thermal, and moisture roughness length in the surface layer, although other schemes are available within WRF (Zilitinkevich et al., 2001, Garrat, 1992). Two runs have been performed to assess the effect of SST, the control run, where WRF uses the 0.5 degrees daily Real-Time Global (RTG) Sea Surface Temperature SST field provided by NCEP (Gemmill et al., 2007; ftp://polar.ncep.noaa.gov/pub/history/sst). In the second run, WRF uses the hourly SST data from MIKE 3 simulation; MIKE 3 employs an unstructured mesh, with a horizontal resolution ranging from 0.2 degrees in far-offshore areas to as fine as 0.05 degrees in the coastal areas of the southeastern North Sea.

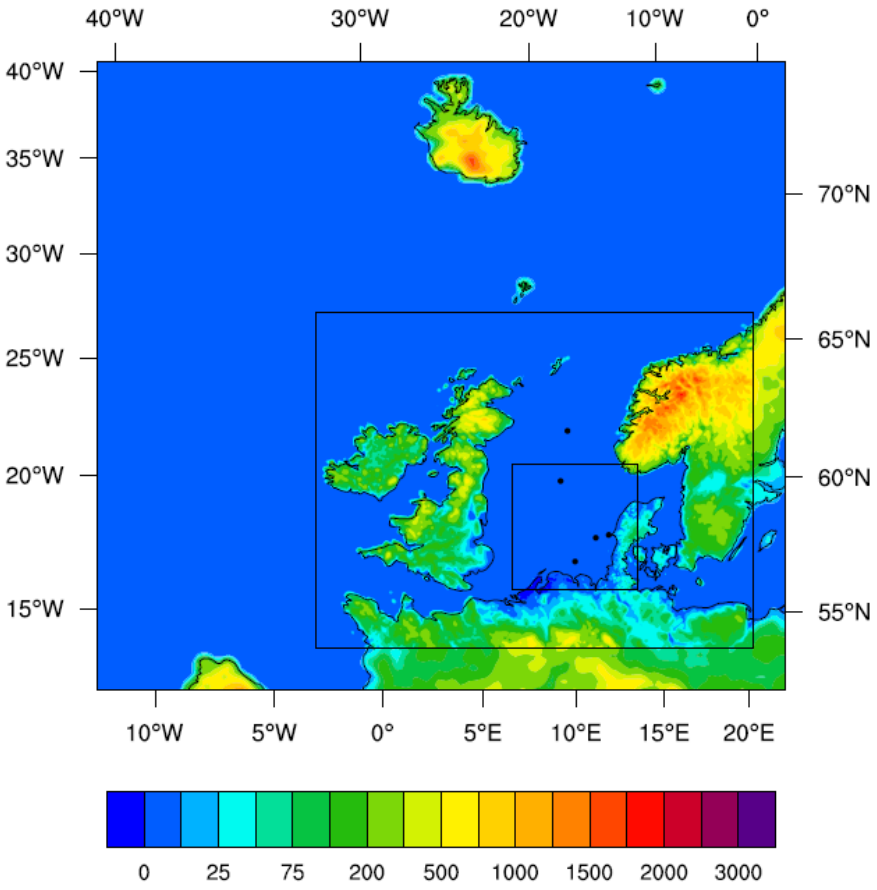

Fig. 1 The model domains that are used in WRF. The horizontal resolution of the first (outermost) domain is 18 km, the second (middle) domain is 6 km, and the third (innermost) domain is 2km. Colorbar represents topography in meters.

5. Results. Impact of model SST on WRF during the November 2011 storm case study

Results of WRF for the two model configurations are assessed at three locations; two of them are offshore locations, named Ekofisk and FINO3. The third location is a nearshore location at Horns Rev (Mast-8). The use of modelled high resolution SST presented slight variation on the atmospheric model results. Wind speed variations were on the order of up to 2 m/s (~10 %) while air temperature of about 0.5^{o} C (~5 %). The largest differences in results were found in the coastal location (Horns Rev). Figures 2 to 4 show time series of WRF and measurements (when available) of wind speed, wind direction, air temperature and sea surface temperature for the three locations.

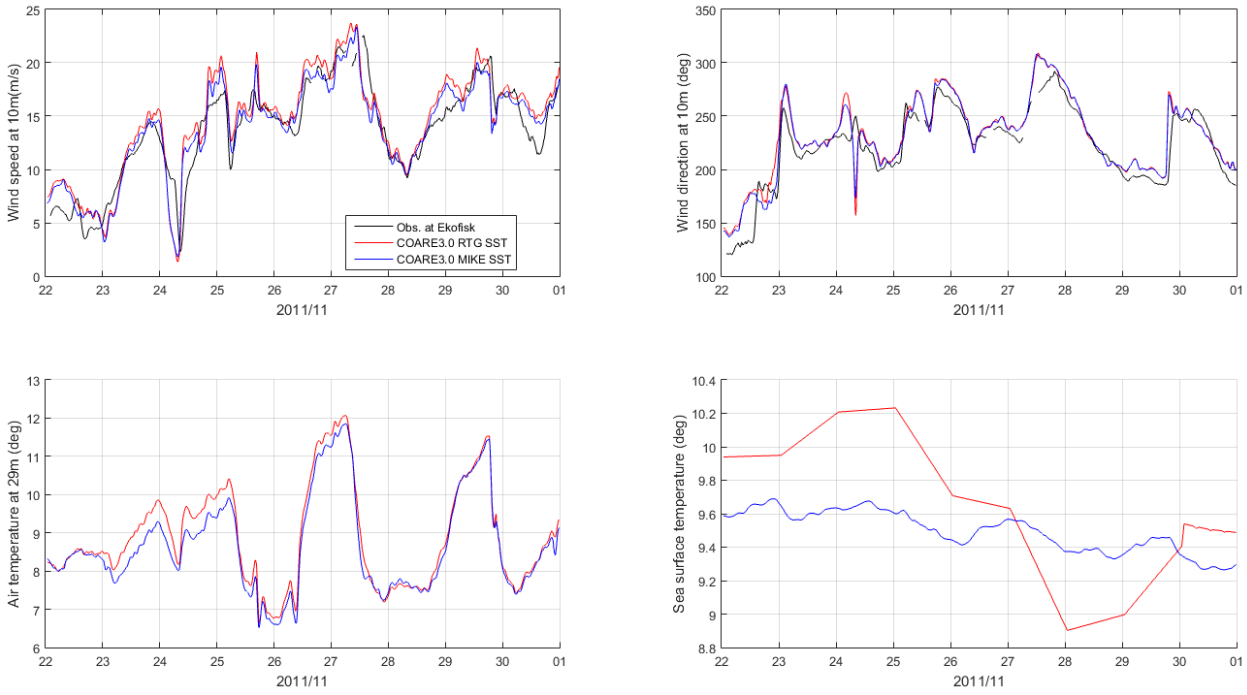

Figure 2. Time series at Ekofisk of wind speed (top left), wind direction (top right), air temperature (bottom left) and sea surface temperature (bottom right).

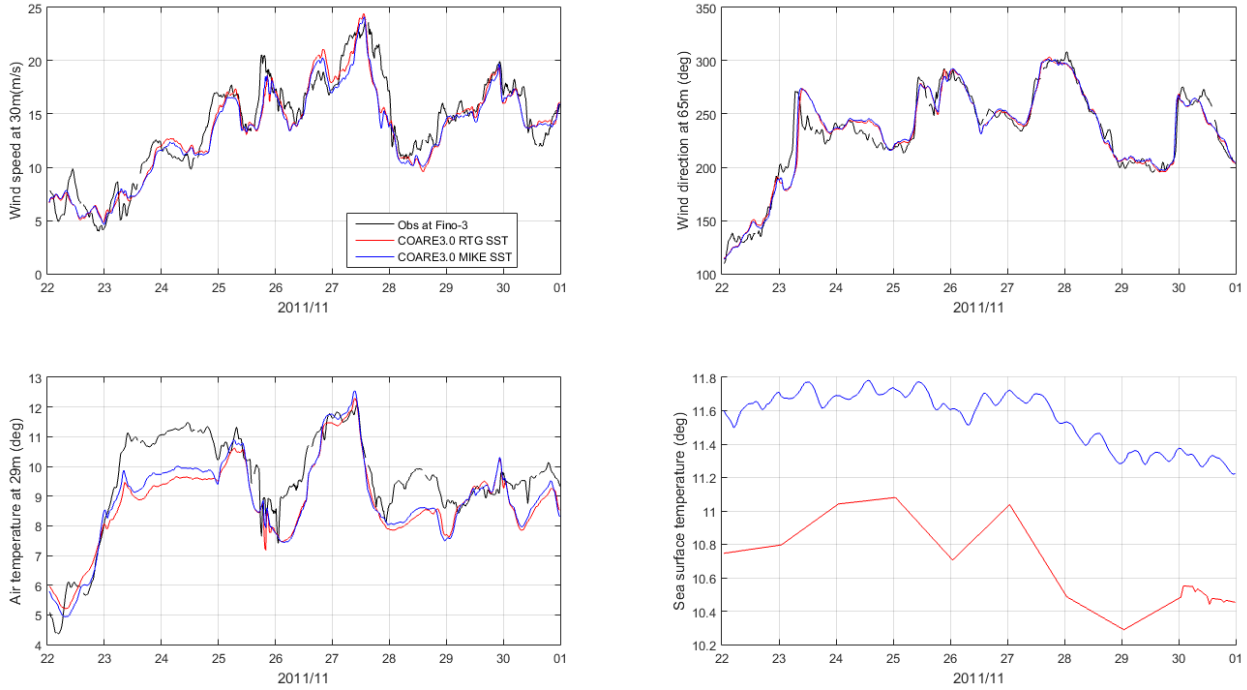

Figure 3. Time series at FINO3 of wind speed (top left), wind direction (top right), air temperature (bottom left) and sea surface temperature (bottom right).

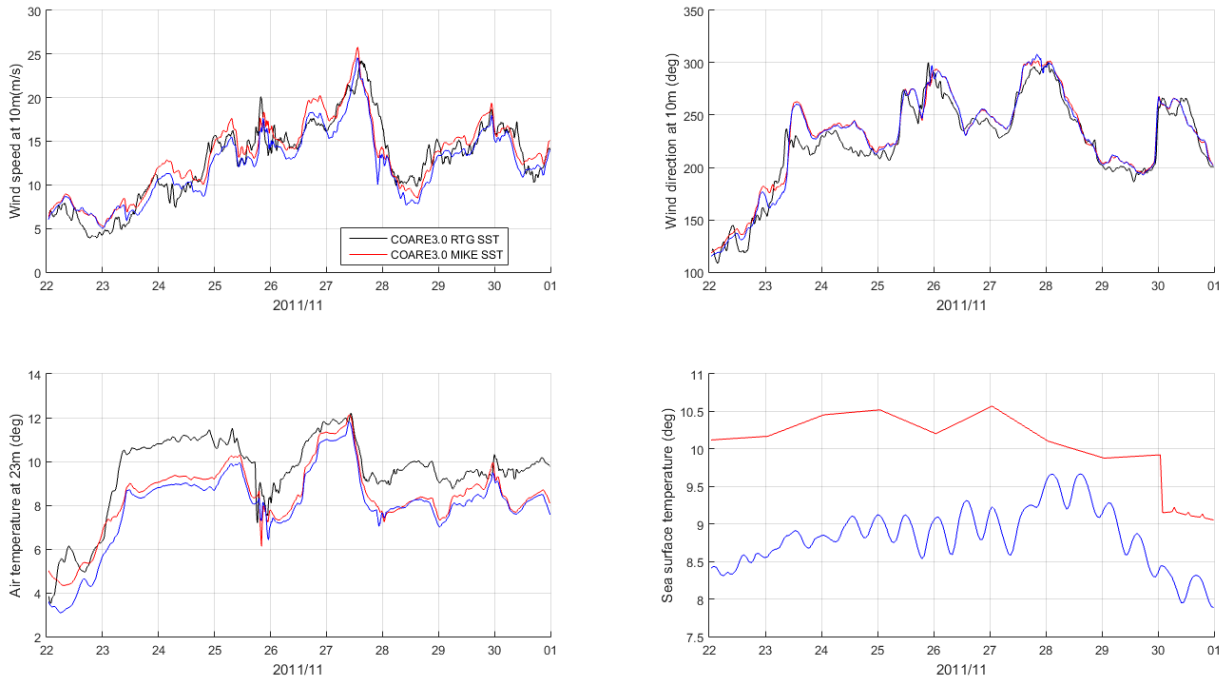

Figure 4. Time series at Horns Rev mast-8: wind speed (top left), wind direction (top right), air temperature (bottom left) and sea surface temperature (bottom right).

Figure 5 shows the time series of differences between WRF results using standard SST and MIKE SST at the three locations, for wind speed, wind direction, air temperature and sea surface temperature, respectively. The largest difference in wind speed is seen at Horns Rev, which is related to the large difference in SST. These SST differences at HR show high frequency oscillations not observed in far-offshore locations.

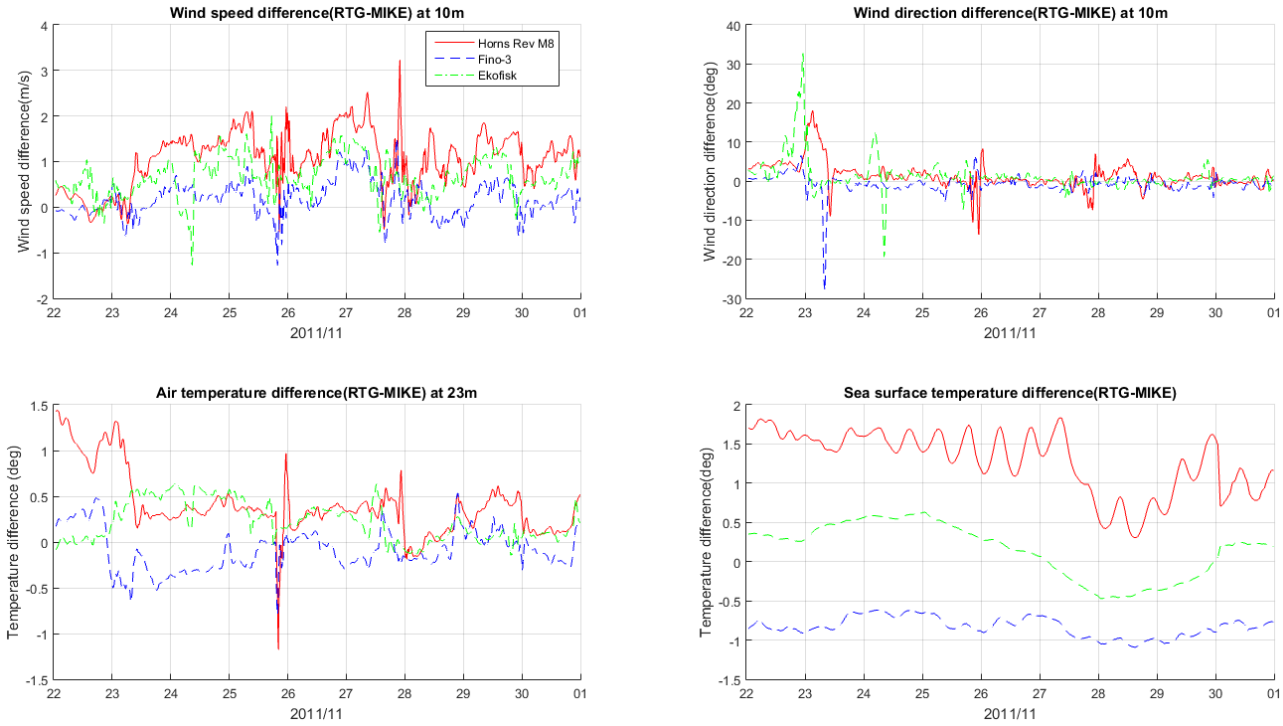

Figure 5. Time series of differences of WRF results when using daily (RTG) and hourly (MIKE) SST. Top right: difference on wind speed. Tor right: difference on wind direction. Bottom left: difference on air temperature. Bottom right: difference on sea surface temperature.

6. Further analysis. Larger diurnal SST events

Diurnal SST warming becomes evident when the surface wind is weak and insolation is strong. Recent observations using satellite data and advanced instruments have revealed that a large diurnal SST rise occurs over wide areas in a specific season, and in an extreme case the diurnal amplitude of SST exceeds 5 deg (Kawai and Wada, 2007).

The storm of November 2011 presented only small diurnal variations of SST, thus a methodology to identify some cases of larger diurnal warming has been implemented. The domain chosen is the area around Denmark, 52^{o}-60^{o} N and 2^{o}-16^{o} E. The 6-year long dataset of hourly SEVIRI SSTs was used, and in order to identify large diurnal warming the criteria were:

i) day-time SST anomaly exceeding 10 from the foundation SST (defined as the temperature of the water column free of diurnal temperature variability) of the previous night, assumed to represent well mixed conditions,
ii) occurring in more than 7 neighbouring grid points to ensure extended spatial coverage. For the latitudes of interest, a SEVIRI grid cell has approximate dimensions of 5.56*3.2 km, equal to an area of 17.8 km^2, thus diurnal warming events covering areas larger than 124.5 km^2 were identified.

Due to the cloud contamination, only SEVIRI SSTs with quality flag from 3 to 5 were used to avoid low quality retrievals. In principle, cloud coverage prevents retrieval of SST but when a pixel is party cloud covered, an SST retrieval can be obtained but it will be of ambiguous quality due to the presence of cloud which tends to lower the SST value.

6.1 Identification of large warming events from SEVIRI SST

Seven cases of large warming were identified, reaching up to 6^{0}. They mostly occurred during spring and summer of 2006, 2008, 2009 and 2010. Some of these large events are shown in Figure 6 and Figure 7 where white areas indicate regions either fully cloud covered or with high chances of cloud contamination and therefore are discarded. The top row of each figure shows the SEVIRI SST anomaly fields at 4 am, 18 pm and at the time of highest warming. The bottom row shows the QuikSCAT 10-m wind speed at approximately 6 am and 6 pm. What is seen in both figures is that early morning SST shows no difference compared to the foundation temperature, assumed to represent well mixed conditions.

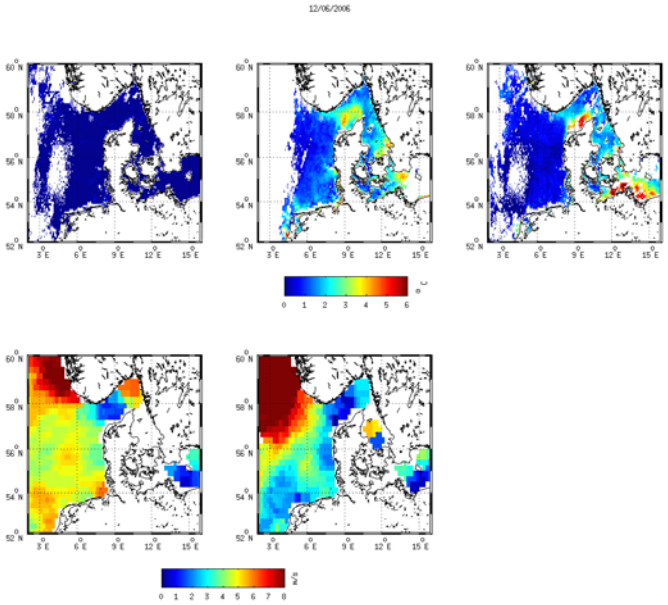

Figure 6. The largest warming event, 12/06/2006. The top row shows SST anomaly fields at 4:00, 18:00 and 11:00. The bottom row shows QuikSCAT wind speed at 6:00 and 18:00.

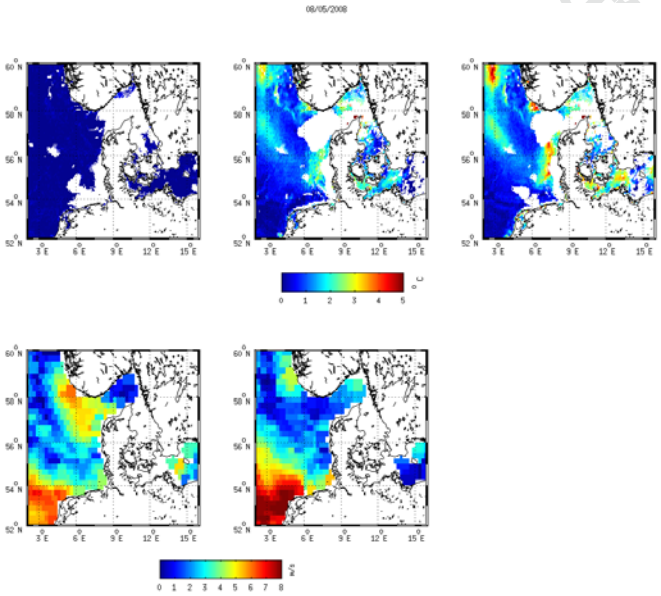

Figure 7. Diurnal warming event on 08/05/2008. The top row shows SST anomaly fields at 4:00, 18:00 and 15:00. The bottom row shows QuikSCAT wind speed at 6:00 and 18:00.

In both cases, the early morning wind fields show relatively low winds at various parts of the domain. The top, right panel in both figures shows the peak warming at 11:00 and 15:00 correspondingly. Up to 5 degrees increase in SST compared to the foundation temperature were recorded in both cases and the areas of warming correspond well with the areas of low morning wind speeds. Increased SST anomalies persist as late as 18:00 (top middle panels in both figures), and the time coincident surface wind fields (middle bottom) show very low wind speeds where the warm SST areas are located. Note that in both cases, warming is not constrained at coastal areas but also observed in offshore locations.

6.2 Optimal Interpolation of hourly SST

Since SEVIRI SSTs are obtained from an infrared instrument, cloud covered regions are not observed and appear as data-free areas in the retrieved hourly SST field. As such, SEVIRI SSTs cannot directly be used to hourly update the SST boundary conditions in WRF due to the gaps in spatial coverage. To overcome this, the optimal interpolation (OI) method used to generate the North Sea/Baltic Sea Reanalysis SST from DMI was used, as described and validated in Høyer and She (2007). Two more satellite SST products, namely the PathFinder Advanced Very High Resolution Radiometer (AVHRR) and the ENVISAT Advanced Along Track Scanning Radiometer (AATSR) Reprocessed for Climate (ARC), were used for the gap-filling procedure to obtain optimally interpolated, hourly SST fields.

For each of the 24 hourly SSTs obtained during the days with high diurnal warming, the OI scheme was used along with the supplementary SSTs from AVHRR and AATSR to fill the gaps due to cloud cover and low quality of retrievals.

Figure 8 shows an average temperature between 16 ^{0}C and 18 ^{0}C in the coastal areas around Denmark at 4:00. By around 13:00, extended areas have warmed up to more than 20 ^{0}C, and this is still the case for the 14:00. By 23:00, despite the obvious decrease of temperature in the warmed up areas, SST has not yet reached to the early morning values.

While during the event of 12/06/2006 extended areas warmed up during the day, on the 08/05/2008 a warm patch off the west coast of Denmark appeared on the SST field as shown in Figure 9. The morning field shows a temperature of 13^{0}C, increasing to more than 16^{0}C at 13:00, and decreasing down to 14^{0}C at 23:00.

These figures are the outcome of optimally interpolating the hourly SEVIRI SST and as such can be used for the hourly update of SST in WRF.

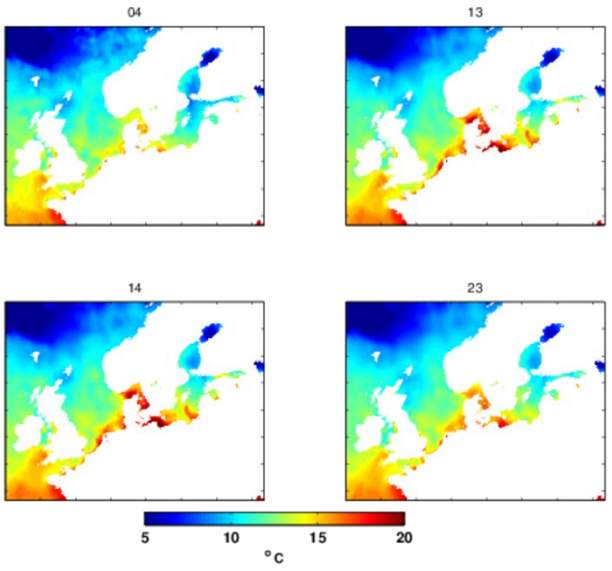

Figure 8. Example of the OI SST for the warming event occurring on June 12, 2006. The numbers above each panel indicate the hour.

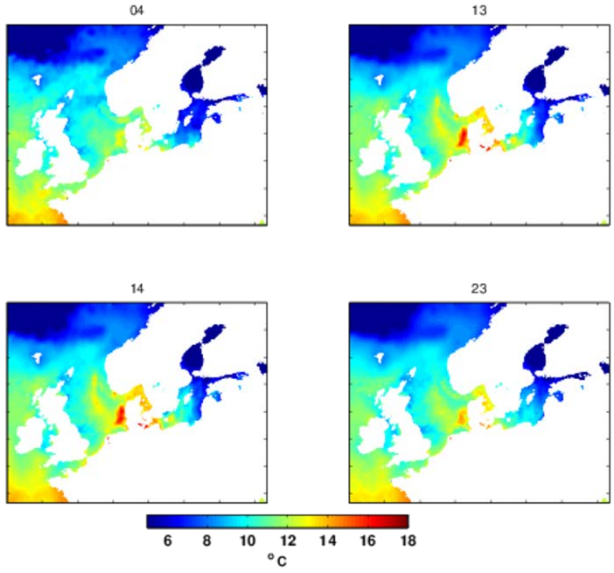

Figure 9. Example of the OI SST for the warming event occurring on May 8, 2008. The numbers above each panel indicate the hour.

7 Discussion

The implementation of MIKE 3 presented good results in terms of the sea surface temperature, and although some bias with the satellite data was obtained (see deliverable D1.15) the model allow us to assess the impact of high resolution SST in the atmospheric model WRF. Several researchers have shown that the imposition of an hourly surface forcing is essential to reproduce diurnal variations in a numerical model (e.g., Weller and Anderson, 1996; Bernie et al., 2005). Although validation for diurnal SST variations has not been performed, it has been

shown by other authors (Price et al. 1987; Webster et al., 1996) that the diurnal SST variation depends primarily on wind speed and solar radiation, proposing empirical models to evaluate the diurnal amplitude of SST. These models show that for winds larger than 10 m/s diurnal variations are lower than 0.5^{o} C, in agreement with the MIKE 3 results.

The response of WRF to the SST from MIKE 3 was mainly observed in the air temperature, and with some effect on wind speed at the coastal location. The difference seems to be due to the different SST mean, not the magnitude of temporal oscillations of the SST input. It seems that the small daily variations in SST are not of significance for the storm case tested (November 2011). The high frequency differences at the coastal location seem to have a tidal origin, due to their semidiurnal frequency. The identification of six cases with large warming diurnal events has shown that they occurred during low wind conditions and, although significant impact of using a high resolution SST could be expected, this will not have a direct impact in extreme wind conditions.

However, the results show that the mean of SST is an important parameter for storm intensity. This brings the question of the quality of SST used, while the default WRF SST data has a spatial resolution of 0.5 degree (about 50 km) other higher resolution products (resolution of 5 – 3 km) could potentially outperform and provide a better SST forcing to the atmospheric modelling during storms.

It has to be noted that a coupling with a short coupling interval (1 - 3 h) between an atmospheric and ocean model can produce diurnal ocean variations (Danabasoglu et al., 2006). However, as pointed out by Kawai and Wada (2007), even if correct diurnal SST variations are supplied to an atmospheric model as a lower boundary condition, the model may not correctly respond to the diurnal variations of SST without appropriate heat flux parameterizations. These atmospheric parameterizations also need to be improved in order to study air-sea interaction on a diurnal time scale.

Selected cases of large increase of the SST during the day have been identified from the analysis of 6 years of hourly SST fields. This daily increase of SST is expected to result in increased heat fluxes, which are not potentially resolved by the WRF model due to the lack of increased temporal resolution of the SST in the model. To evaluate the impact of large SSTY variations on the modelled fluxes and the derived wind speed fields, the hourly satellite SSTs have been optimally interpolated to fill gaps due to cloud coverage. Thus, they are now ready to be implemented in WRF. Results regarding the biases arising in the heat fluxes and the wind field will be available in the near future.

8 Future atmospheric modelling

Seven selected cases of diurnal warming will be modelled in WRF. The run period will be the day before, to allow spin up time in the model, and finishes the day after the day of large diurnal SST variability. Thus, a total of 3 days will be modelled in each case.

For three of the cases, hourly SST fields will be used in WRF for the entire run period, i.e. 3 days. For the remaining 4 cases, hourly SST fields will be used only in the day of the large warming event, while the day before and after 1 daily field will be used.
In all cases, to avoid spurious SST values in the hourly OI field of 00 hours, i.e. the first OI field produced in each interpolation round, the DMI reanalysis is used instead. From 01 onwards, the actual SEVIRI OI fields are used.

To obtain comparable results, the selected cases will be also modelled using the standard daily SST OI field, used operationally in WRF at DTU Wind Energy. This product is available from 1981 at 0.25 degrees spatial resolution. In addition, to evaluate the impact of using a high resolution daily OI SST specifically developed for the Northern European Seas, the DMI Reanalysis SST will be also used in WRF for the same cases. Prior to the final modelling experiments, sensitivity tests in WRF will be performed regarding the selection of Planetary Boundary Layer (PBL) and surface schemes, only using the hourly SST OI fields.

Another set of experiments will be performed to find out whether the spray effect is important for modelling the mid-latitude storm systems. In comparison with the modelling of the tropical cyclones, the effect from the spray, being on the heat flux on the initialization of the storm/hurricane, or being on the stress transport, might be not the same in the cases of the mid-latitude storms.

Acknowledgements

The BMWi (Bundesministerium fuer Wirtschaft und Energie, Federal Ministry for Economic Affairs and Energy) and the PTJ (Projekttraeger Juelich, project executing organization) are greatly acknowledge for providing FINO platform data. Dong energy is also acknowledge for providing Horns Rev measurements data. Authors thank other X-WiWa members for support and contributions.

References

Andreas, E.L., DeCosmo, J., 2002. The signature of sea spray in the HEXOS turbulent heat flux data. Boundary-layer Meteorology 103, 303-333.

Andreas, Persson and Hare, 2008. A bulk turbulent air-sea flux algorithm for high wind, spray conditions. J. Phys. Oceanogr. 38:1581-1596.

Andreas, E.L., Mahrt, L., Vickers, D., 2015. An improved bulk air-sea surface flux algorithm, including spray-mediated transfer. Quarterly Journal of the Royal Meteorological Society 141, 642-654.

Barenblatt, G.I., Chorin, A.J., Prostokishin, V.M., 2005. A note concerning the Lighhthill "sandwich model" of tropical cyclones. Proc. Natl. Acad. Sci. USA., 11148-11150.

Bellenger H., and J. P. Duvel: An analysis of ocean diurnal warm layers over tropical oceans. J. Climate, 22, 3629-3646, 2009.

Bellenger H., Y. N. Takayabu, T. Ushiyama, and K. Yoneyama: Role of diurnal warm layers in the diurnal cycle of convection over the tropical Indian Ocean during MISMO. Mon. Wea. Rev. 138, 2426-2433, 2010.

Bernie, D.J., Woolnough, S.J., Slingo, J.M., Guilyardi, E., 2005. Modeling of diurnal and intraseasonal variability of the ocean mixed layer. Journal of Climate 18, 1190-1202.

Chiang, T.L., Wu, C.R., Oey, L.Y., 2011. Typhoon Kai-Tak: an ocean's perfect storm. Journal of Physical Oceanography 14, 221-233.

Danabasoglu, G., Large, W.G., Tribbia, J.J., Gent, P.R., Briegleb, B.P., McWilliams, J.C., 2006. Diurnal coupling in the tropical oceans of CCSM3. Journal of Climate, 2347-2365.

Donlon C., Robinson I, Casey KS, Vazquez-Cuervo J, Armstrong E, Arino O, and co-authors: The Global Ocean Data Assimilation Experiment High-resolution Sea Surface Temperature Pilot Project. Bull. Am. Met. Soc. 88(8), 1197-1213, 2007.

Eastwood S., Le Borgne P., Péré S., and D. Poulter: Diurnal variability in sea surface in the Arctic. Rem. Sens. Environ. 115, 2594-2602, 2011.

Emanuel, K. (2003). A Similarity Hypothesis for Air–Sea Exchange at Extreme Wind Speeds. J. Atmos. Sci. **60**, 1420-1428.

Fairall, C. W., Bradley, E. F., Hare, J. E., Grachev, A. A., & Edson, J. B. (2003). Bulk parameterization of air-sea fluxes: Updates and verification for the COARE algorithm. Journal of climate, 16(4), 571-591.

Fan, Y., Lin, S.J., Held, I.M., Yu, Z., Tolman, H.L., 2012. Global ocean surface wave simulation using a coupled atmosphere-wave model. Journal of Climate 25, 6233-6252.

Garratt, J. R., 1992. The atmospheric boundary layer, Cambridge atmospheric and space science series. Cambridge University Press, Cambridge, 416, 444. p.

Gemmill, W., Katz, B., Li, X., & Burroughs, L. D. (2007). The daily Real-Time, Global Sea Surface Temperature–High Resolution Analysis: RTG_SST_HR1.

Høyer, J. and She, J: Optimal interpolation of sea surface temperature for the North Sea and Baltic Sea. J. Mar. Sys. 65 (1-4), 176-189, 2007.

Iacono, M. J., Delamere, J. S., Mlawer, E. J., Shephard, M. W., Clough, S. A., & Collins, W. D. (2008). Radiative forcing by long -lived greenhouse g
radiative transfer models. Journal of Geophysical Research: Atmospheres (1984–2012), 113(D13).

Janssen, J.A.M., 1997. Does wind stress depend on sea-state or not? - a statistical error analysis of HEXMAX data. Boundary-layer Meteorology 83, 479-503.

Janssen, P.A.E.M., 1997. Effect of surface gravity waves on the heat flux, Technical Memorandum 239. ECMWF, Reading.

Jarosz, E., Mitchell, D.A., Wang, D.W., Teague, W.J., 2007. Bottom-up determination of air-sea momentum exchange under a major tropical cyclone. Science 315, 1707-1709.

Jensen, R.E., Cardone, V.J., Cox, A.T., 2006. Performance of third generation wave models in extreme hurricanes, 9th International wind and wave workshop, Victoria, B.C.

Kain, J. S., & Fritsch, J. M. (1993). Convective parameterization for mesoscale models: The Kain-Fritsch scheme. In The representation of cumulus convection in numerical models (pp. 165-170). American Meteorological Society.

Karagali I., Hoeyer J., and C. B. Hasager: SST Diurnal Variability in the North Sea and the Baltic Sea. Rem. Sens. Env. 112 (513), 1195-1225, 2012.

Karagali, I. and J.L. Høyer: Characterisation and quantification of regional diurnal SST cycles from SEVIRI. Oc. Sci., 10, 745-758, 2014.

Kawai, Y., Wada, A., 2007. Diurnal sea surface temperature variation and its impact on the atmosphere and ocean: a review. Journal of Oceanography 63, 721-744.

Kudryavtsev, V.N., 2006. On the effect of sea drops on the atmospheric boundary layer. Journal of Geophysical Research 111, C07020.

Le Borgne P., Legendre G., and S Péré: Comparison of MSG/SEVIRI and drifting buoy derived diurnal warming estimates. Rem. Sens. Env. 124, 622-626, 2012.

Liu, Guan and Xie (2012): The wave state and sea spray related parameterization of wind stress applicable from low to extreme winds. Journal of geophysical research, vol 117, C00J22, doi:10.1029/2011JC007786.

Mahrt L., Vickers D., Frederickson P., and K. Davidson (2003): Sea-surface aerodynamic roughness. J. Geophys. Res.: Oceans **108**, 3171, doi:10.1029/2002JC001383, C6.

Merchant, C. J., Filipiak, M. J., Le Borgne, P., Roquet. H., Autret. E., *et al.*: Diurnal warm-layer events in the western Mediterranean and European shelf seas. Geophysical Research Letters, 35, L04601, 2008.

Minnett, P., and Kaiser-Weiss, A.: Near-surface oceanic temperature gradients. GHRSST Discussion document, 2012.

Moon, I.J., Ginis, I., Hara, T., Thomas, B., 2007. A physics-based parameterization of air-sea momentumflux at high wind speeds and its impact on hurricane intensity predictions. Monthly Weather Review 135, 2869-2878.

Mueller, J.A., Veron, F., 2009. Nonlinear formulation of the bulk surface stress over breaking waves: feedback mechanism from air-flow separation. Boundary-layer Meteorology 130, 117-134.

Nakanishi, M., & Niino, H. (2006). An improved Mellor–Yamada level-3 model: Its numerical stability and application to a regional prediction of advection fog. Boundary-Layer Meteorology, 119(2), 397-407.

Pielke, R.A., Lee, T.J., 1991. Influence of sea spray and rainfall on the surface wind profile during conditions of strong winds. Boundary-layer Meteorology 55, 305-308.

Price, J., Weller, R., Bowers, C., and M. Briscoe: Diurnal Response of Sea Surface Temperature Observed at the Long-Term Upper Ocean Study (34 N, 70W) in the Sargasso Sea. J. Geophys. Res., 92(C13), 14480-14490, 1987.

Sanford, T.B., Price, J.F., Girton, J.B., Webb, D.C., 2007. Highly resolved observations and simulations of the ocean response to a hurricane. Geophysical Research Letters 34, L13604.

Thompson, G., Rasmussen, R. M., & Manning, K. (2004). Explicit forecasts of winter precipitation using an improved bulk microphysics scheme. Part I: Description and sensitivity analysis. Monthly Weather Review, 132(2), 519-542.

Vickers D., Mahrt L., and E.L. Andreas: “Formulation of the Sea Surface Friction Velocity in Terms of the
Mean Wind and Bulk Stability”. J.Appl.Met.Clim. 54, 691–703.

Ward, B.: Near-surface ocean temperature. J. Geophys. Res. 111, C02004, 2006.

Webster P. J., Clayson C. A., and J. A. Curry: Clouds, radiation, and the diurnal cycle of sea surface temperature in the Tropical Western Pacific. J. Clim. 9, 1712-1730, 1996.

Weller, R.A., Anderson, S.P., 1996. Surface meteorology and air-sea fluxes in the western equatorial Pacific warm pool during the TOGA coupled Ocean-Atmosphere Response Experiment. Journal of Climate 9, 1959-1990.

Wu, Rutgersson, Sahlée and Larsén., 2015. The impact of waves and sea spray on modeling storm track and development. Tellus, In revision.

Zhang, Perrie and Li, 2006. Impact of waves and sea spray on mid-latitude storm structure and intensity, Monthly Weather Review. 134:2418 -2441.

Zilitinkevich, S. S., Grachev, A. A., & Fairall, C. W. 2001. Reasoning and Field Data on the Sea Surface Roughness Lengths for Scalars. Journal of the Atmospheric Sciences, 58(3), 320-325

4. Appendix D

M1.7 Subroutines for the estimation of the sea spray heat fluxes and 2D fields of sea spray heat fluxes effect on the roughness

Xiaoli G. Larsén, Rodolfo Bolaños, Mark Kelly and more

As explained in the Interim report, this report is to be updated. The work related has started but it is seen not as the major effort we should put on to for the moment as other components are more urgent to be developed. In this report, we show the work we did so far and plans for the next project phase.

Without considering explicitly the spray effect, in WRFV3.5, there are 5 options for the descriptions of z0, zT and zq, where zT and zq are functions of z0. The algorithms were collected in the X-WIWA note (Larsén 2013) that has been distributed to everyone. Here is a copy of it:

1 Roughness lengths over water as in WRFV3.5, mynn scheme

There are 5 descriptions for the set of z_0, z_{0T} and z_{0q}.

1.1 option 0

z_0, z_{0T} and z_{0q} are all from COARE3.0 (Coupled Ocean-Atmosphere Response Experiment) [1]. These are bulk flux algorithms with wind speed at 10 m at neutral conditions, $U_{10,n}$, in the range of $0 - 20$ ms^{-1}. For rough flow $R_r > 2$, where R_r is the roughness Reynold's number:

$$R_r = \frac{z_0 u_*}{\gamma} \tag{1}$$

with γ the kinematic viscosity of the standard atmosphere, the set of algorithms are:

$$z_0 = \frac{\alpha u_*^2}{g} + \frac{0.11\mu}{u_*} \tag{2}$$

where the Charnock parameter α increases linearly from 0.011 at $U_{10,n} = 10$ ms^{-1} to 0.018 at $U_{10,n} = 18$ ms^{-1} and remains constant for lack of better information beyond this limit.

$$z_{0T} = z_{0q} = min(1.1 \cdot 10^{-4}, 5.5 \cdot 10^{-5} R_r^{-0.6}) \tag{3}$$

Eq.s 3 and 1 suggest a decreasing drag for heat with wind speed in the medium speed range.

For smooth flow $R_r \leq 2$:

$$z_{0T} = 5.5 \cdot 10^{-5} R_r^{-0.6} \tag{4}$$

$$z_{0q} = 0.2 \cdot \gamma / max(u_*, 0.1) \tag{5}$$

1.2 option 1

z_0 is from [2] with some update to adjust a small bias in z_0 (from WRF note *module sf mynn.F*). The original algorithm as in [2] is: $z_0 = 10 \cdot \exp -10/(u_*^3)$, which was based on the relation of the drag coefficient with wind speed from lab experiments of [3]. The corrected algorithm is:

$$z_0 = (1-(\frac{u_*}{1.06})^{0.3})(\frac{0.011u_*^2}{g}+1.59\cdot 10^{-5})+(\frac{u_*}{1.06})^{0.3}\cdot\left(10\exp\left(-9.5u_*^{-1/3}\right)+\frac{0.11\cdot 1.5\cdot 10^{-5}}{u_*}\right) \quad (6)$$

A maximum and a minimum value of z_0 was set by [2] based again on the lab data from [3]: $2.85 \cdot 10^{-3}$ and $0.125 \cdot 10^{-6}$ m.

The descriptions of z_{0T} and z_{0q} are the same as eq. 3, where the expressions are validated with wind speed up to 20 ms^{-1}.

1.3 option 2

The description of z_0 is eq. 6.

The formulations for z_{0T} and z_{0q} are modified from the original Garratt-Brutsaert model to fit the COARE/HEXMAX data ([1]).

$$z_{0T} = z_0 \cdot \exp\left(2 - 2.48 \cdot R_r^{0.25}\right) \quad (7)$$

$$z_{0q} = z_0 \cdot \exp\left(2 - 2.28 \cdot R_r^{0.25}\right) \quad (8)$$

The ranges of both z_{0T} and z_{0q} are set to be $[2 \cdot 10^{-9},\ 5.5 \cdot 10^{-5}]$ m, where the lower limit is as ECMWF.

1.4 option 3

The algorithms are from [4] where z_0 is a function of wave steepness:

$$z_0 = 1200 \cdot h_s(h_s/L_p)^{4.5} \quad (9)$$

where h_s is the significant wave height and L_p is the wave length associated with the peak of the wave spectrum.

WRF uses the formulations for h_s from [4] for fully developed seas where $C_p/U_{10} = 1.14$ or $C_p/u_* = 28$ (which correspond to moderate wind speed range):

$$h_s = 0.0248 \cdot U_{10}^2 \quad (10)$$

and

$$L_p = gT_p^2/(2\pi) \quad (11)$$

where T_p is the dominant wave period and it is calculated as

$$\begin{aligned} T_p &= 0.729 \cdot U_{10}, \quad U_{10} > 0.1\ ms^{-1} \\ &= 0.1, \quad U_{10} \leq 0.1\ ms^{-1} \end{aligned} \tag{12}$$

The upper and lower limits of z_0 as those in [2](option 1) are used, namely $2.85 \cdot 10^{-3}$ and $0.125 \cdot 10^{-6}$ m.

The formulations for z_0 and z_q are as eq.s 3, 4 and 5.

1.5 option 4

z_0 is described by Charnock as in [1] and 1.1, z_{0T} and z_{0q} are from [5].

For rough flows where $Re > 0.1$, here $Re = max(R_r, 0.1)$

$$z_{0T} = z_0 \cdot \exp\left(-\kappa \cdot (4\sqrt{Re} - 3.2)\right) \tag{13}$$

and

$$z_{0q} = z_0 \cdot \exp\left(-\kappa \cdot (4\sqrt{Re} - 4.2)\right) \tag{14}$$

At the same time, z_{0T} and z_{0q} constrained between $2 \cdot 10^{-9}$ and $6 \cdot 10^{-5}$ m.

For smooth flows where $Re < 0.1$

$$z_{0T} = z_0 \cdot \exp\left(-\kappa \cdot 2\right) \tag{15}$$

and

$$z_{0q} = z_0 \cdot \exp\left(-\kappa \cdot 3\right) \tag{16}$$

where κ is the von Kamen constant 0.4.

Although in [5] the above expressions of z_{0T} and z_{0q} were plotted for Re of about 100, their measurements are in the range $0.4 < Re < 10$, where the highest wind speed is about 10 ms^{-1}.

2 Discussion

[2] pointed out that "the real drag force on surface winds is determined by the time-evolving ocean wave spectrum, prediction of which requires a wave model [6]". Rodolfo's report provides a number of parametrization of z_0 through wave parameters.

z_{0T} and z_{0q} at stormy wind strength are less known. We will look into the literatures to decide how to take wave breaking and sea spray into account.

Heat transfer at high winds and our activities and plans

The field experiments as introduced in a series of work lead by Andreas have led to a new unified parameterization for the turbulent air-sea heat fluxes that should be especially useful in high winds because it acknowledges both the interfacial and spray routes by which the sea exchanges heat and moisture with the atmosphere. Andreas and DeCosmo (2002) suggested that the spray effects are most evident in the latent heat flux data, where spray contributes roughly 10% of the total turbulence flux in the winds of 10 m/s and between 10 and 40% in the winds of 15-18 m/s. Many numerical studies have used the spray mediated transfer functions for sensible and latent heat developed by Andreas et al. (2008) to examine how the im-

plementation of the spray effect affects the drag coefficient and wind field for storm and hurricane wind strength (e.g. Liu et al. 2012, Wu et al. 2015).
This is a relevant topic for this project, both for atmospheric and wave modeling.
One of the purposes is to find out whether the spray effect is important for modeling the mid-latitude storm systems. In comparison with the modeling of the tropical cyclones, the effect from the spray, being on the heat flux on the initialization of the storm/hurricane, or being on the stress transport, might be not the same in the cases of the mid-latitude storms.
Within the time frame, the following issues are considered, some parts have already started (e.g. 1). Depending on the progress and project resources, we will need to readjust the tasks during the time.

1. Currently, as a standard, z0T and z0q are parameterized through z0, or similarly, the relation of Cd and CH and CE is used. There is no consensus on their exact dependence (e.g. Larsén et al. 2004, Zeng et al. 1998, kalogiros and Wang 2011). What is the case over the waters close to Denmark? We will examine all measurements available (we have turbulence measurements at Horns Rev, water temperature and SST) and revisit some measurements from the Baltic Sea, to see if the data quality is good enough for such a study and if under certain conditions they can be used, how the results are and how the results be further applied.
2. Sensitivity tests in real and ideal modes for storm cases: using the schemes as in WRF, with modification of the wind speed dependence.
3. Sensitivity tests with spray mediated transfer.

References

Andreas, Mahrt and Vickers (2014): An improved bulk air-sea surface flux algorithm, including spray-mediated transfer. QJRMS, DOI:10.1002/qj.2424
Andreas, Persson and Hare (2008): A bulk turbulent air-sea flux algorithm for high wind, spray conditions. J. Phys. Oceanogr. 38:1581-1596.
Kalogiros and Wang (2011): Aircraft observations of sea surface turbulence fluxes near the California coast. BLM, 139:283-306.
Kudryavtsev and Makin (2011): Impact of ocean spray on the dynamics of the marine atmospheric boundary layer. BLM. 140 (3), 383-410.
Larsén X. (2013) Notes on the roughness lengths descriptions in WRFV3.5. X-WIWa report.
Larsén, Smedman and Högström (2004): Air-sea exchange of sensible heat over the Baltic Sea. QJRMS. 130:519-539.
Liu, Guan and Xie (2012): The wave state and sea spray related parameterization of wind stress applicable from low to extreme winds. Journal of geophysical research, vol 117, C00J22, doi:10.1029/2011JC007786.
Rastigejev, Suslov and Lin (2012): Effect of ocean spray on vertical momentum transport under high wind conditions. BLM, DOI10.1007/s10546-011-9625-1.
Soloviev and Lukas (2010): Effects of bubbles and sea spray on air-sea exchange in hurricane conditions. BLM. 136:365-376
Wu, Rutgersson, Sahlée and Larsén (2015): The impact of waves and sea spray on modeling storm track and development. Tellus, In revision
Zeng, Zao and Dickinson (1998): Intercomparison of bulk aerodynamic algorithms for the computation of sea surface fluxes using TOGA COARE and TAO data. J. Climate, 11, 2628-2644.

5 Appendix E

Mid-term assessment of the X-WiWa project

2015-08-11

Report
2015

By Xiaoli Guo Larsén

Cover photo: [Text]
Published by: Department of Wind Energy, Frederiksborgvej 399
Request report from: www.dtu.dk
ISSN: [0000-0000] (electronic version)
ISBN: [000-00-0000-000-0] (electronic version)

ISSN: [0000-0000] (printed version)
ISBN: [000-00-0000-000-0] (printed version)

Preface

This report assesses the work that has been conducted within the X-WiWa project for the first half part, from July 2013 to June 2015.

Risø Campus, DTU, 2015

Xiaoli Guo Larsén
Seniorforsker

Overview of the many aspects of the project

In this report we go through the work that has been done within the first half part of the X-WiWa project, with references to the original project proposal and four half-yearly, periodic Interim reports that have been submitted to Energinet.dk.

The assessment has been shown through power point at our mid-term meeting to all project members, see appendix. Similar items are shown and explained here.

As stated in the proposal, what we in the current project aim at developing and what we expect to achieve is copied here:

A.1.2 Expected findings

The major objective of X-WiWa is to develop a new model system for accurate forecasting of waves and wind during storms by coupling the most advanced atmospheric, wave and oceanic models. The new model system is expected to forecast wind speed at hub height and nearshore significant wave heights with an accuracy of 90%. In order to achieve this final objective, we expect to develop:

- A novel modelling system for wind and waves during storm conditions in the Danish coastal zones, through the coupling of the atmospheric, wave and ocean models.
- Coupling approaches for the atmospheric and wave models, here particularly the Weather Research and Forecast (WRF) model and its Large Eddy mode (WRF-LES), and the MIKE by DHI wave and ocean models, for the purpose of extreme wave and wind forecast.
- An improved description of wind field during storm conditions in the coastal zone due to the coupling of the atmospheric and wave models. The wind description includes wind speed and shear at the hub height, strong wind duration, turbulence intensity and their spatial distribution.
- An improved description of storm wind field by better parameterization of heat transfer from the ocean.
- The extreme wind atlas in the Danish coastal zone.
- The description of the wave field in the coastal zone during storm conditions due to improved wind input.
- A better understanding of the impact of coastal waves on the wind profiles.

For these, the project is running in the right direction, details are shown in the following.

For the “Technical Development”, we are making progress in the proposed four major activities:

- Coupling the atmospheric model WRF with wave model MIKE 21 SW
- Bridging between mesoscale modeling and microscale modeling
- Incorporating ocean modeling
- Making the model outputs user-friendly

Among these, we have been and are currently working actively with the first three, while the fourth is expected to be most relevant at later stage of the project.

The proposed project structure was as follows:

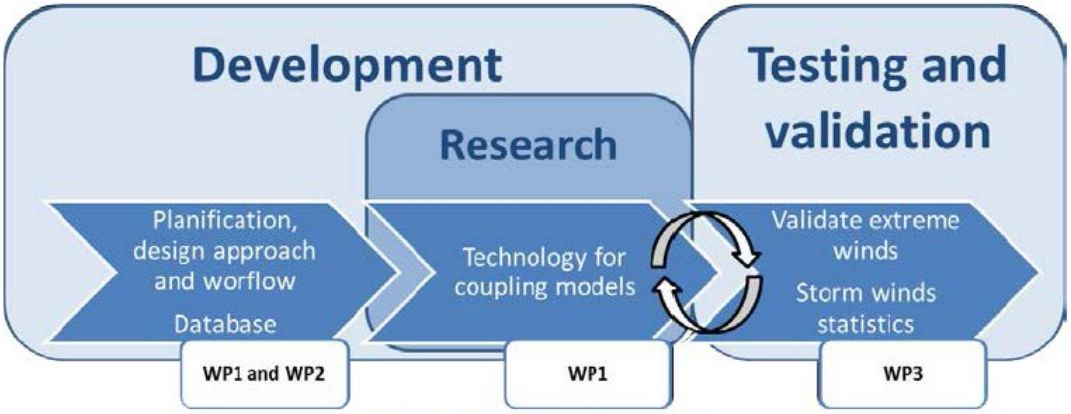

Figure A: Project structure.

This turns out to be a helpful structure. Based on this structure, the project has been developed following:

- Building up a database (for validation and analysis useful for understanding and improving the modeling),
- Building up the coupling system,
- Data validation,

which fits the PERT diagram in the proposal, showing the inter-relations between the three work packages WP1 (modeling), WP2 (observational database) and WP3 (validation and application):

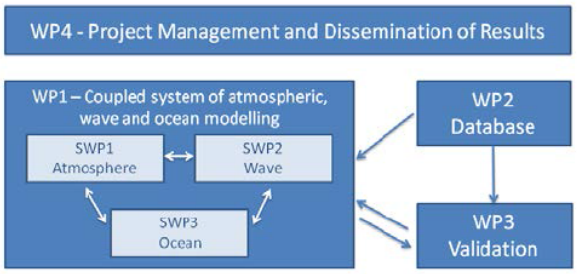

Figure C. PERT Diagram. The inter-relations between work packages WP1 (modelling), WP2 (observational database) and WP3 (validation and application), and the 3 sub-work packages within WP1.

As shown in all periodic Interim reports, we have been performing as scheduled, with slight modification of the order of some activities, based on our knowledge learnt during the project. This small modification includes the experiments of using WRF-LES and the study of sensible heat that have been slowed down (see details in Interim report IV), because a series of technical issues related to other parts of the modeling need to be clarified. We have successfully delivered Milestones and Deliverables as stated in the Gantt Chart:

D1.1 The offline and online coupling systems
M1.4 Subroutines in MIKE SW to estimate the parameters to be transferred to the atmospheric model
D2.1 & M2.1 X-WiWa database
D3.1 Validation of the selected storms through the roughness length technique in the coupled modeling system
D1.15 Report on the implementation of the ocean model MIKE 3
D1.16 Sensitivity report of the heat effects during extreme events
M4.1 Mid-term assessment (This report)

Milestone M1.7 (Subroutines for the estimation of the sea spray heat fluxes and 2D fields of sea spray heat fluxes effect on the roughness) is however delayed intentionally. We submit along the Interim report phase 4 a preliminary draft of the report but its content will be updated. The delay was complicated by several facts. One is the observation through our experiments that the numerical effect on the atmospheric modelling related to the input of roughness length is quite insensitive. The focus is therefore put to examine the numerical code how this is happening. Another reason is that the experiments related to heat transfer are currently being put under effort through various input of SST and there still needs evaluation on this topic. It is foreseen to make better sense to draw conclusions on these matters first and then start examining the spray effect.

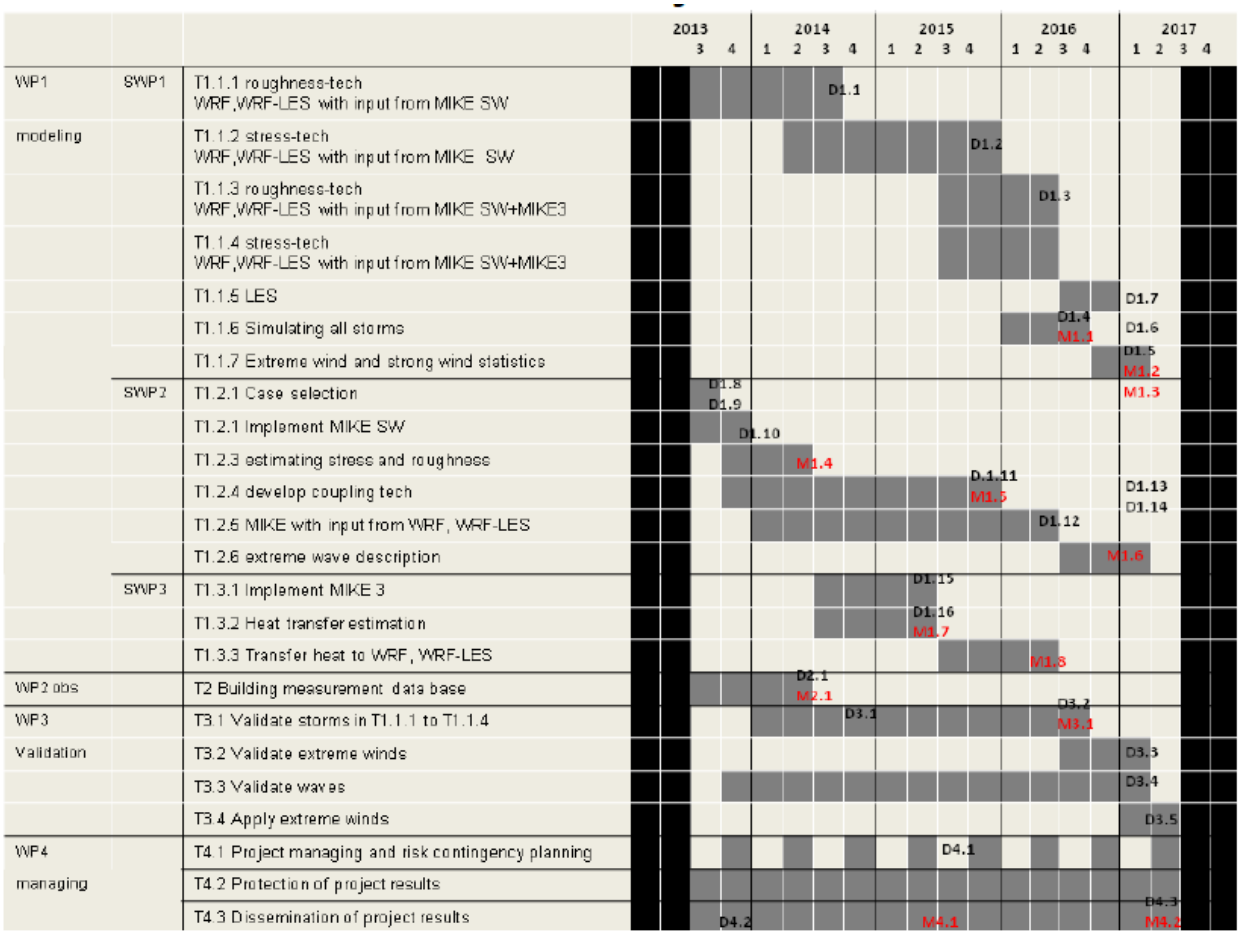

The measurement database has been built and documented in D2.1 and M2.1. It has been kept updated with new measurements (see Interim report IV).

The development of the modeling system has been taken the following sequence:

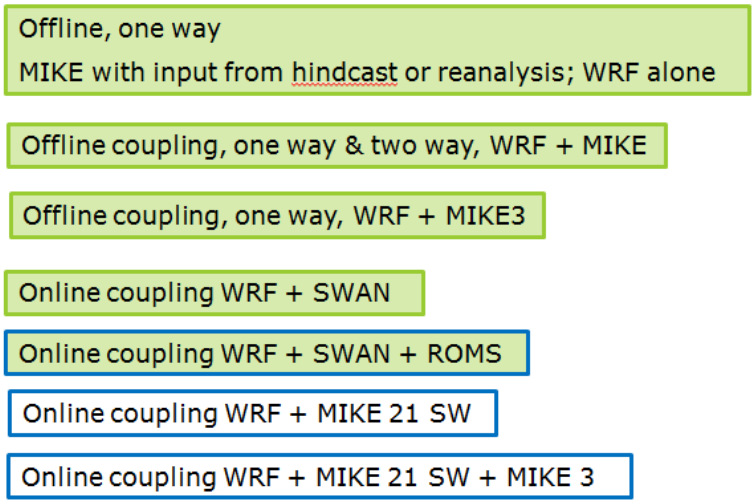

The green boxes are the ones that have been successfully developed. The blue outlined boxes are those we are still developing and under assessment to see if the offline version may suffice.

For those finished parts in the modeling system, we are making efforts on improving the numerical and physics calculation of key parameters.

Model validation has been done constantly to all experiments with available data. This is our major focus for the moment. This step is essential in judging if the technics that have been developed are good enough to resolve the physics problems and it gives feedback on how we should continue and improve the modeling system.

There have been quite a number of research notes, reports and presentations done by members of the project, among them:

- Bolaños R. 2013. Coupling atmospheric-wave-ocean models, state of the art. X-WiWa report.
- Bolaños R. and Kofoed-Hansen (2015) Small fetch and extreme winds wave growth in MIKE 21 SW. X-WiWa report. 24 pages
- Du J. An overview of the model couplers for X-WiWa, technical report, 5 pages.
- Du J., Larsén X. and Bolaños R.: Preliminary results from nested offline coupling using WRF and MIKE 21 SW. Phd process report
- Jenkins A. D. 2013. WRF-WAM coupling with MCEL. Uni-Computing, X-WiWa report.
- Karagali I. 2015: WRF modeling with satellite SST. X-WiWa report, 6 pages.
- Larsen S. Sea-surface roughness and wave characteristics - the variety of expressions. Uppsala mini air-sea interaction workshop, 16-17th May 2014, Uppsala Sweden (PPT, report)
- Larsén X. G. 2013: Notes on the roughness length descriptions in WRF v3.5.1. X-WiWa report.
- Larsén X. G. 2014: A note on the parametrization of water roughness length and its impact on the wind profile during storms in the coastal area.
- Nielsen J.R. 2013: Technical notes on the WRF-MIKE 21 SW offline coupling. Wiki web site.

- Nielsen J.R., Larsén X. and Bolaños R. 2013: Preliminary results from the offline coupling for a storm case – impact of water roughness length from MIKE 21SW on the WRF simulation. Power Point Presentation.

There have been a number of international conference papers and presentations as well:

- Du J., Larsén X.G. and Bolaños R. (2015) A coupled atmospheric and wave modeling system for storm simulations. Abstract and poster at EWEA Offshore conference March 2015, Copenhagen.
- Bolaños, R., Larsen, X.G., Petersen, O.S., Nielsen, J.R., Kelly, M., Kofoed-Hansen, H., Du, J., Sørensen, O.R., Larsen, S.E., Hahmann, A., Badger, M., 2014. Coupling atmosphere and waves for coastal wind turbine design, in: Lynett, P.J. (Ed.), 34th International Conference On Coastal Engineering. Coastal Engineering Research Council, Seoul, Korea, p. 11.
- Larsén X., Du J. and Bolaños, R. (2015): Wind structure during mid-latitude storms and its application in Wind Energy, conference abstract in proceedings, The 4th Hydrology-Atmosphere-Ocean conference, 19 – 21 July, 2015, Shanghai, China.
- Larsen S. Sea-surface roughness and wave characteristics - the variety of expressions. Uppsala mini air-sea interaction workshop, 16-17th May 2014, Uppsala Sweden (PPT, report)
- Larsén X. G. and all X-WiWa members, 2014c: Siting of offshore wind turbines: extreme wind and waves. Uppsala mini air-sea interaction Workshop, 16-17th May 2014, Uppsala Sweden. PPT.
- Larsén X. G. and all X-WiWa members, 2014d: Siting of offshore wind turbines. Danish Wind Industry Annual Event 2014, R&D Conference, 1st March 2014, Hernning Denmark. PPT and Poster.
- Larsén X.G. and Kruger A. 2014b: Extreme gust wind estimation using mesoscale modeling, in proceedings, EWEA 2014, paper and PPT.

Journal papers:

- Larsén X., C. Kalogeri, G. Galanis and G. Kalos, 2015: A statistical methodology for the estimation of extreme wave conditions for offshore renewable application. *Renewable Energy,* 80, 205 – 218